Time-Resolved ExB Probe Measurement of Hall Thruster Plasma

Mitsuki Shimomura

A thesis

submitted in partial fulfillment of the requirements for the degree of

Master of Science

University of Washington

2025

Committee:

Justin Little

Bhuvana Srinivasan

Program Authorized to Offer Degree:

Aeronautics and Astronautics

University of Washington

Abstract

Time-Resolved ExB Probe Measurement of Hall Thruster Plasma

Mitsuki Shimomura

Chair of the Supervisory Committee:

Justin Little

Department of Aeronautics and Astronautics

Reconstruction of synchronized time-resolved ExB probe measurement is conducted on a Hall-effect thruster operating on krypton at three power levels. The synchronization is implemented with an algorithm based on Fourier transfer functions between the discharge current and ExB probe measurements. The research serves as the baseline for future investigation of time-resolved ion velocity and charge state diagnostics for Hall-effect thrusters. ExB measurement is closely tied to both the ion velocity distribution function and charge-state distribution. The obtained reconstructed ExB probe signal is analyzed using parametric curve-fitting with the superposition of two Maxwellian distribution functions. The result of analysis qualitatively suggests the presence of temporal and spatial variation of charge-state distribution in the exhaust plasma. Future steps for improvement and further research are mentioned.

Table of Contents

Table of Figures

Acknowledgements

I would like to express my gratitude to Prof. Justin Little, the director of the SPACE Lab at the University of Washington and my faculty advisor. I have received his advice since my undergraduate program, and his support has been very helpful for me to pursue research and knowledge in the field of electric propulsion.

Mr. Peter Thoreau from the SPACE Lab helped me tremendously with the experiment and the operation of the thruster. It is thanks to him that experimental data is available for this thesis.

I also would like to express special gratitude and acknowledgement for Prof. John Williams of Colorado State University, the director of CSU Electric Propulsion & Plasma Engineering (CEPPE) Laboratory. I had my first experience in electric propulsion research, more particularly time-resolved diagnostics for Hall thruster plasma, during my undergraduate research internship at Colorado State University in the summer of 2022. The research topic of this thesis was strongly influenced by the knowledge and insights I gained from the experience.

I. Introduction

Background

Hall-effect thrusters (HET) are gradually becoming one of the most mainstream types of electric propulsion systems for Earth-orbiting satellites for the purposes of station keeping, orbit maintenance, etc. The simplicity of the thruster and the ability to achieve high thrust density without space-charge limitations, unlike gridded-ion thrusters, make HETs a promising method of space propulsion for various missions.

The HET consists of an annular acceleration channel parallel to the axial direction, across which the external magnetic field is applied either with electromagnets or permanent magnets, an anode located at the spacecraft-side of the acceleration channel, and a hollow cathode mounted outside the acceleration channel. The anode typically also serves as the propellant injector. A circulatory flow of electrons is formed in the annular acceleration channel and ionizes the incoming propellant neutrals via collisions. The flow of electrons, forming an electron cloud, also serves as the virtual grid, accelerating the propellant ions via electrostatic acceleration. The outgoing flow of ions is neutralized by a portion of the electron flow from the hollow cathode, thus preventing a charge build-up. Shown below is a simplified schematic of a typical HET:

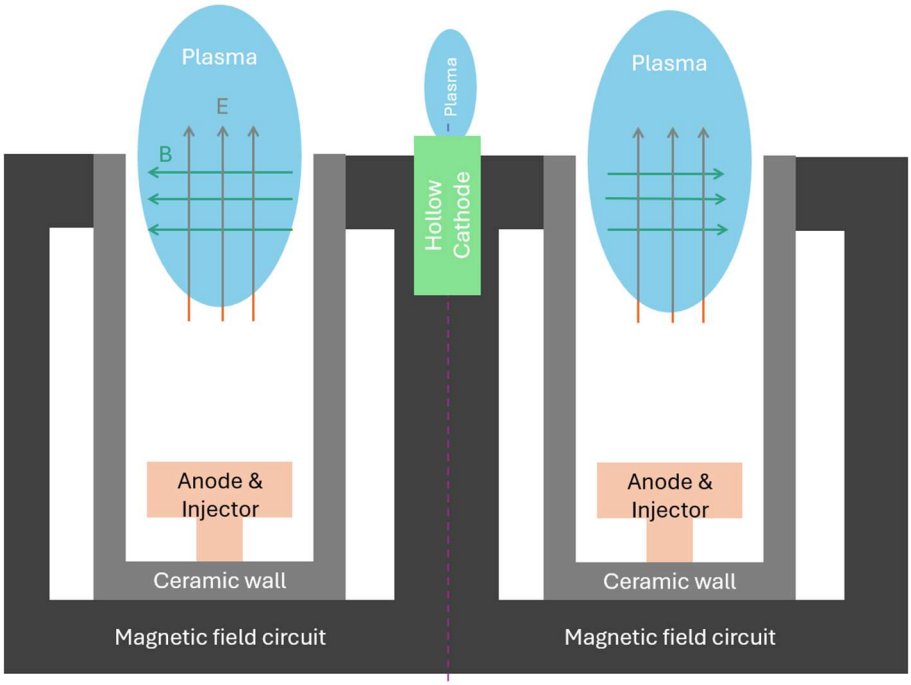

Figure I-1: A simplified schematic of a Hall-effect thruster with a centrally mounted hollow cathode.

Some of the detailed physics behind the behavior of HETs is yet to be fully understood, especially when it comes to the time-resolved behavior of plasma. Here, time-resolved refers to time scale small enough to resolve some meaningful temporal change of plasma and thruster parameters, as opposed to time-averaged understanding in which the temporary variation of the plasma or thruster parameters is neglected. It is already widely understood through experimental measurement and theoretical considerations that the discharge current of HETs shows oscillatory behavior, the low-frequency (~30kHz) oscillation called the breathing mode being the dominant oscillation mode. The breathing mode oscillation causally propagates to various parameters of the exhaust plasma, including ion energy, ion velocity, ion flux, electron temperature, and so on. The physical correspondence between the breathing mode oscillation in the discharge current and the plasma parameters allows numerical or machine-learning approaches to model the

relationship between the discharge current and the plasma parameter measurements made by probes, as an example via transfer functions in the Fourier space.

As the use of HETs and other electric propulsion devices increases in scale and number, there are pressing research needs in the field of Hall thruster development and relevant plasma diagnostics. One of such needs is the reduction of testing time and cost. Conventionally, newly developed thrusters go through life testing in vacuum chambers to ensure that they meet the lifetime requirement (1,000~10,000 hours), which can take more than a year along with a large amount of propellant. The price of xenon, the most common propellant for HETs, is currently remarkably high and easily affected by international relations. Lifetime testing consumes a significant amount of time and resources, and simplifying and accelerating the lifetime testing processes can lead to a significant improvement in the development efficiency of HETs, allowing developers to further improve their HET designs within limited time and resources, for example through rapid iterative design and testing.

One approach to achieving this objective is to explore a closer combination of experimental data with computational models, thus allowing developers to obtain useful insights on their design with less time- and resource- consuming experimental processes. In constructing a computational model of the exhaust plasma, the ion velocity distribution function (IVDF) along with the charge-state distribution plays a key role, and obtaining the relevant time-resolved measurement will be beneficial for constructing a computational model that accurately models the behavior of the thruster and the plasma.

Objective and impact of this work

1. Research objective

This research aims to test and establish the methodology of experiment and analysis to obtain the time-resolved, synchronized measurement of a Hall thruster exhaust plasma using an ExB probe, a simple electrostatic probe widely used for time-averaged measurements. Furthermore, the research aims to obtain the time-resolved variation of charge-state distribution in correspondence to the breathing mode, based on the analysis of the synchronized time-resolved ExB measurement. The technical explanation regarding the ExB probe can be found in the proceeding section.

Essentially, the research first aims to apply the method of transfer function hitherto applied to other types of time-resolved measurement to the time-resolved ExB probe signal combined with the measurement of discharge current and obtain the synchronized measurement. Secondly, the well-established methodology of analyzing the time-averaged ExB signal for charge-state distribution is applied at each time step of the obtained time-resolved measurement, thus yielding the time-resolved understanding of the charge-state distribution of the Hall thruster exhaust plasma.

2. Research impact

The ExB probe is a common and simple experimental equipment with a well-established methodology to analyze the ion velocity and charge-state distributions. While laser induced fluorescent (LIF) is capable of IVDF measurement with high spatial and temporal resolutions, LIF requires complex experimental apparatus, and measurement on a plasma with multiple charge states typically requires multiple laser frequencies, further complicating the experimental

apparatus. Enabling time-resolved measurement with the ExB probe can broaden the research field for many researchers at low cost.

Gaining time-resolved understanding of ion velocity and charge state distributions of the Hall thruster exhaust plasma can give further insight into Hall thruster physics, thruster simulation modeling and design optimization for higher performance of the thruster, including lifetime.

Literature Review

The time-resolved measurement of the Hall thruster exhaust plasma with an ExB probe, or the time-resolved measurement of ion velocity distribution in general over multiple charge states is a novel research field, and no past publication of time-resolved ExB-probe or charge-state measurement for Hall thrusters has been identified. This section will first summarize the past research related to conventional time-averaged velocity or charge-state profiles of Hall thruster exhaust plasma. The section will also summarize the research related to the measurement of time-resolved ion velocity distribution and other highly relevant plasma characteristics, namely the ion energy distribution, using different experimental methodologies. Finally, the suggested implications of ion velocity oscillations on the HET design and performance are also mentioned.

1. Time-averaged ExB measurement of HET exhaust plasma

Shastry [1] summarizes the best practices for time-averaged ExB-probe measurement on Hall thruster exhaust plasma and for the numerical analysis of the measured data. Several variations of the method to determine the current fractions of each observed charge state are introduced, and curve-fitting with a Gaussian profile as the distribution profile is introduced as one of the methods to numerically determine the current fraction. The CEX correction model originally

developed by Anderson [2] to correct the raw measurement accounting for the alteration of charge-state distribution along the travel path of the ions between the thruster and the probe due to charge-exchange (CEX) reactions is simplified and used as the CEX correction model for the xenon plasma. The experiment was performed on a 6-kW laboratory Hall thruster operating on xenon, and the experimental results showed that the CEX correction has a significant impact on the calculation of the thruster efficiency parameters.

Reid [3] at the University of Michigan performed ExB-probe measurements on the exhaust plasma of a 6-kW Hall thruster operating on xenon propellant at various operating conditions as well as axial and angular positions. The author reports that the comparison of corrected measurements from multiple axial probe positions confirms the high accuracy of the CEX correction method. The experimental results show the relative increase in the fraction of multiply charged ions corresponding to the separate, controlled increase of discharge voltage and propellant mass flow rate. The author also reports that the charge-state distribution varies with angular positions, while the measurement along the channel centerline captures the characteristics spatially averaged over the plasma plume well.

Kim [4] studied the charge-state distribution in conventional and cylindrical Hall thrusters operating on xenon and found that the plasma in cylindrical Hall thrusters have higher percentage of multiply charged ions. Kim attributed the increase in thrust and specific impulse to the increased percentage of multiply charged ions. Kim also noted that the increase in multiply charged ions results in an increase in discharge current, which increases the power consumption of the thruster.

2. Time-resolved HET exhaust plasma characteristics

The technique to synchronize multiple sensor readings for HET experiments was first pioneered by Lobbia [5] to synchronize the readings from sensors various positions around the thruster. The technique played a fundamental role in understanding the oscillatory dynamics of the HET plasma [6]. Lobbia applied the FFT data-fusion technique to spatiotemporal measurement taken with a dual Langmuir probe. The experimental results confirmed the presence of global oscillation in the exhaust plasma parameters, dominated by the breathing mode oscillation. Lobbia also introduced the technique to compute the transfer functions corresponding to smaller segments of the measured data and compute the average transfer function to reduce chaotic (non-oscillatory) components from the measurement.

Chaplin [7] performed a time-resolved measurement of the ion velocity distributions in a 12.5-kW Hall thruster using LIF measurements. The author applied the method of Fourier transfer function to the LIF measurement and the measurement of discharge current and cathode-to-anode voltage to reconstruct the time-resolved ion velocity distribution function of the exhaust plasma. The reconstructions with the discharge current and with the cathode-to-anode voltage measurement showed equivalent results. The author reports a strong oscillatory correspondence of the peak of the ion velocity distribution to the “breathing mode” oscillation of the discharge current, the amplitude of the peak velocity oscillation being roughly on the same scale as the mean peak velocity.

Romadanov [8] also experimentally studied the time-resolved ion velocity distribution with LIF and the obtained IVDF showed oscillatory behavior in both height and group velocity. The study was performed only for singly charged ions. Romadanov found the “surprising result” that the time-resolved diagnostics with LIF is faces physical limitations when the exhaust plasma exhibits high-amplitude oscillatory behavior, because the excitation cross-section of ions is

affected by the high-amplitude oscillation of electron temperature and other plasma parameters, suggesting that LIF diagnostics for time-resolved IVDF faces large uncertainties in such conditions.

Ortega [9] conducted an investigation combining experimental and simulation methods into the time-resolved behavior of Hall thruster exhaust plasma and found that in certain operating conditions, the large-amplitude oscillatory behavior of the thruster and the plasma is the primary driving factor for the erosion of the front pole cover of the thruster, which can have design and lifetime implications on the thruster.

In 2022, an unpublished research was conducted into the application of Fourier transfer function, reservoir computing, and shadow-manifold interpolation to the reconstruction of time-resolved electrostatic analyzer measurement was conducted by Mr. Seth Thompson, Prof. John Williams and myself at the Colorado State University to obtain the time-resolved ion energy distribution function of the exhaust plasma of a 200-W class Hall thruster. The obtained results showed good agreement with Chaplin [7], indicating a clear correspondence of peak ion energy oscillations to the breathing mode and demonstrating the capability of numerical methods to derive time-resolved measurement from a conventional plasma probe. The reconstructed time-resolved ion energy distribution function is shown below:

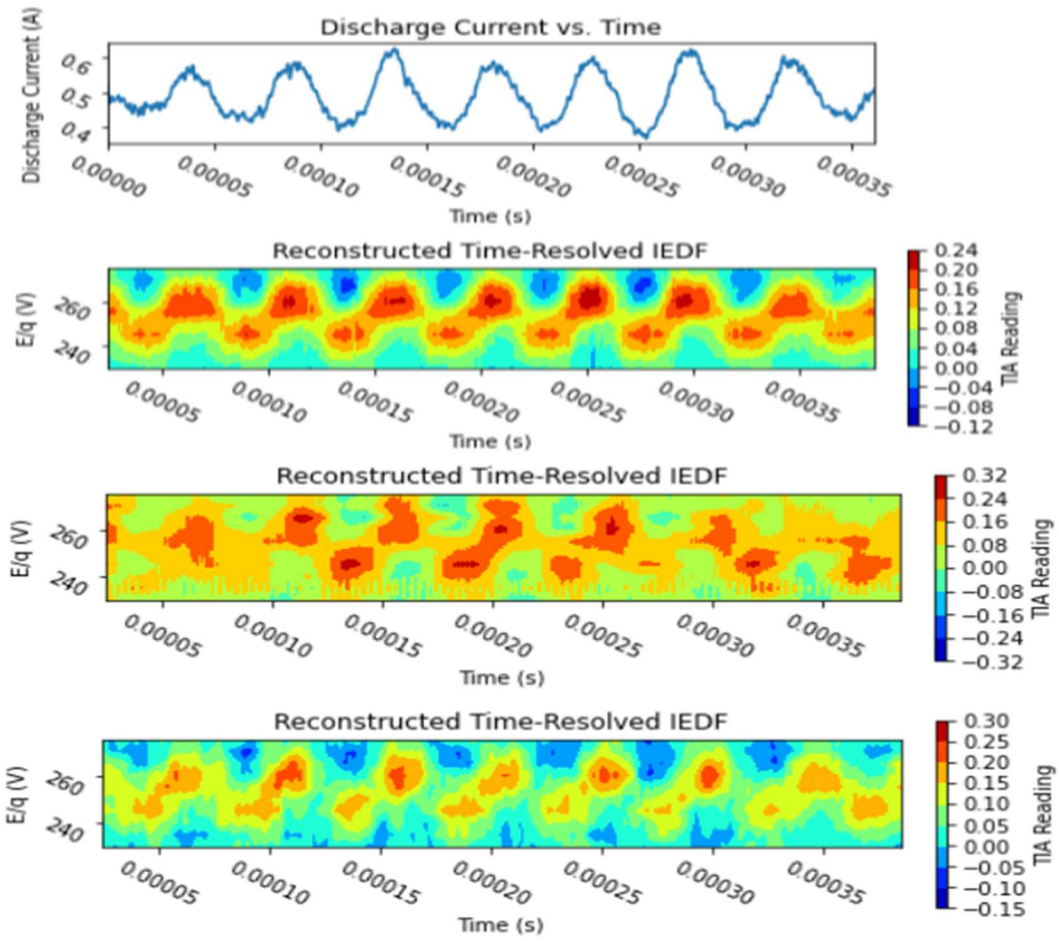

Figure I-2: Reconstructed time-resolved ion energy distribution function synchronized to the discharge current (top). The methods used are, from the 2nd plot: Reservoir computing, FFT ransfer functions, and shadow manifold interpolation.

II. Physical & Numerical Theories

This chapter summarizes the physical models, including simplifying assumptions, used to model and analyze the nature of the exhaust plasma. Many of the models were derived from past relevant research identified through literature review. Furthermore, the chapter summarizes the theoretical backgrounds behind the numerical methods applied to the collected raw data to obtain the desired data, the time-resolved ion velocity distribution function.

1. ExB Probe Theory

The ExB probe (also known as the Wein probe) is a probe utilized to measure the intensity of ion current corresponding to a specific ion velocity. The probe consists of a collimator, which prevents non-axial ion flow from entering the probe, the electrodes, magnets and the detector, which converts the incoming ion flow to current signal. The electrodes are connected to a variable DC voltage source. The electric field applied by the electrodes and the magnetic field applied by the magnets are perpendicular to each other, and both are perpendicular to the longitudinal direction. Figure II-1 below shows the schematics of the ExB probe:

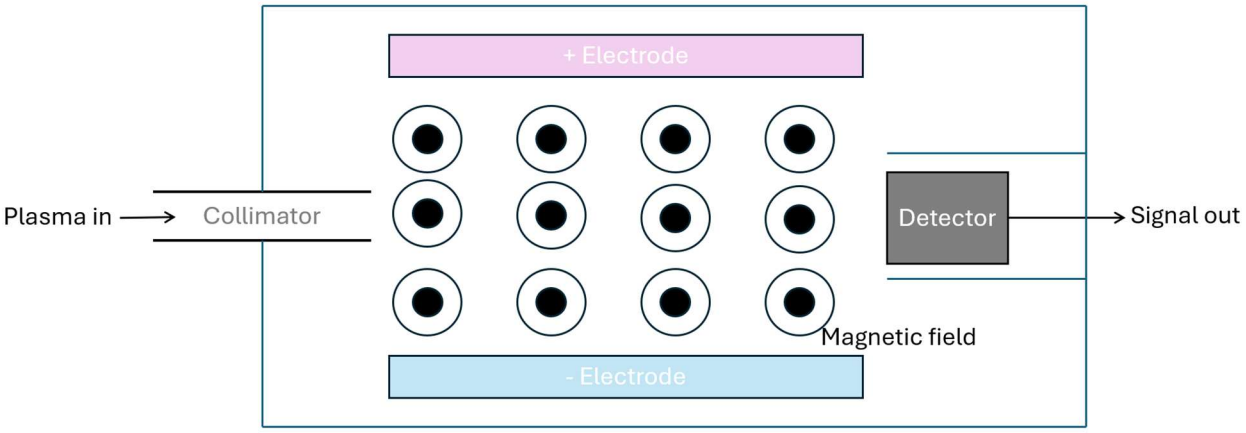

Figure II-1: A conceptual drawing of a ExB probe.

The basic working principle of the ExB probe is that it uses the Lorentz force as the filtering force:

$$\boldsymbol{F} = q(\boldsymbol{E} + \boldsymbol{v} \times \boldsymbol{B})$$

Because the ions that passed the collimator would continue to travel in a straight trajectory and reach the detector only if the force exerted to the ion is zero, one can notice that the probe can be used to measure the ion current intensity corresponding to an arbitrary ion velocity by varying the voltage difference between the electrodes. The ions that pass through the collimator and the electromagnetic filtering collide with the detector. Charge exchange with electrons occur as ions collide with the detector, and results in electric current corresponding to the filtered ion current. Mathematically:

$$\frac{E}{B} = v_{ion}$$

which leads to:

$$\frac{V_p}{Bd} = v_{ion}$$

where V_p denotes the voltage difference applied to the electrodes of the probe.

Therefore, the collected current has the following ideal relationship [[10]]:

$$I_{ExB} = eZ_i n_i u_i A_c$$

2. *Simplifying plasma assumptions*

In order to obtain a useful understanding of the fundamental nature of the exhaust plasma from the limited experimental data, several simplifying yet reasonable assumptions were made regarding the exhaust plasma.

First, it was assumed that impurity in the plasma was negligible. The plasma inside the experimental facility contains ions and neutrals of atomic species different from that of the propellant, due to plasma-material interaction with the thruster components or with the facility, or due to impurity in the propellant gas supplied to the thruster. However, it was assumed that any signal measured beyond the detectable threshold corresponds to propellant ions.

Second, it was assumed that the specie-wise (i.e., *charge-state-wise*) group velocities correspond to the respective charge state of the ions, ions with higher charge states having higher group velocities than ions with lower charge states. In reality, an ion that ionized or underwent a charge-exchange interaction in a location different from the nominal location of the Hall current would experience an amount of acceleration different from the rest of the plasma. However, it was assumed that such phenomena do not affect the general ordering of the group velocities.

3. *Charge-exchange model*

As the plasma consisting of ions with different charge states travel from the thruster exit toward the probe, two ions with different charge states can undergo a collision, and at certain probabilities, the two ions exchange charge (CEX). Because the primary interest in this investigation is in the composition of the plasma generated by the thruster, the current collected by the probe needs to be corrected to calculate the species-specific ion current at the thruster exit, by accounting for the CEX processes along the plasma travel path.

In this investigation, the simplified CEX developed by Shastry [1] which is derived by simplifying the CEX model derived by Anderson [2] assuming a one-dimensional beam accelerated by the same potential, is used for the correction of probe current for time-averaged measurement. The correction model is as follows:

$$\frac{j}{j_0} = \exp\left(-n_0 \sigma z\right)$$

Here, j denotes the measured ExB collector current, and j_0 denotes the current corrected at the thruster exit. σ, n_0, and z denote the charge exchange cross section, neutral number density, and the distance between the thruster exit plane and the probe, respectively. Shastry et. al. constructed the CEX correction model for Xenon plasma. In this investigation, the charge exchange cross section experimentally obtained by Hause [11] is applied to Shastry's model to derive the CEX correction model for the Krypton exhaust plasma. The charge-exchange cross section for Hall thruster Krypton plasma as reported by Hause is as follows:

$$\sigma_1 = 80.7 - 14.7 \log(V_d)$$

$$\sigma_2 = 44.6 - 9.8 \log\left(V_d\right)$$

The cross-section areas are obtained in the units of $10^{-20}\ m^2$. Combining, the CEX correction model for Krypton is expressed as follows:

$$\left(\frac{j}{j_0}\right)_{Kr1+} = \exp(-n_0\sigma_1 z)\,, \sigma_1 = \{80.7 - 14.7\log(V_d)\} \times 10^{-20}$$

$$\left(\frac{j}{j_0}\right)_{Kr2+} = \exp(-n_0\sigma_2 z)\,, \sigma_2 = \{44.6 - 9.8\log(2V_d)\} \times 10^{-20}$$

Shastry experimentally showed that the CEX effects due to the thruster neutrals are negligible [1]. Utilizing this assumption, the only CEX effect to be considered here is due to the presence of neutral background gas, and its number density can be calculated by the ideal gas law based on the base pressure measurement of the vacuum chamber.

4. Transfer-function analysis

As the ExB probe measurement is taken for each measurement value of the probe bias voltage which corresponds to the ion velocity values, there needs to be a mechanism in place to relate the time-resolved behavior of the probe measurement to the state of the thruster to reconstruct the overall time-resolved ion velocity distribution function.

To achieve this, fast-Fourier transform (FFT) is applied to both the probe measurements and the discharge current measurements. Then, for each bias voltage of interest, the transfer function between the Fourier-transformed probe measurement and the Fourier-transformed discharge current measurement is computed. Finally, the obtained transfer functions corresponding to the set of bias voltage values are multiplied with the Fourier transform of a shared single exemplary segment of the discharge current measurement, and then converted back using inverse Fourier transform, thus generating a set of reconstructed ExB probe measurements

in-phase with the shared discharge current measurement and all other reconstructed signals. The generated signals are combined together to reconstruct the time-resolved ion velocity distribution function of the plasma.

Mathematically, this algorithm can be described as follows:

$$I(u,t)_{recon} = F^{-1}\left[\frac{\tilde{I}_{ExB}(u,\omega)}{\widetilde{I_d}(u,\omega)} * \widetilde{I_{d,samp.}}(\omega)\right]$$

where:

- $I(u,t)_{recon}$: Reconstructed ion current as a function of ion velocity u and time t
- F^{-1}: One-dimensional inverse Fourier transformation, with regard to temporal frequency
- $\tilde{I}_{ExB}(u,\omega)$: Fourier transform of time-resolved ExB measurement for ion velocity u
- $\widetilde{I_d}(u,\omega)$: Fourier transform of time-resolved discharge current measurement taken in-phase with the ExB measurement for ion velocity u
- $\widetilde{I_{d,samp.}}(\omega)$: Fourier transform of the exemplary time-resolved discharge current measurement

It is important to note that the fraction $\frac{\tilde{I}_{ExB}(u,\omega)}{\widetilde{I_d}(u,\omega)}$ is the Fourier transfer function between the ExB probe signal and the discharge current at the bias voltage corresponding to ion velocity u. While the mathematical expression above remains true, the transfer function to be multiplied with the Fourier transform of the sample discharge current is obtained as the average of multiple transfer functions calculated using segments of measurements at the same bias voltage in this investigation, as the ExB probe measurement contains a large amount of noise. The specific implementation of this algorithm is described in the proceeding chapter.

The assumption behind this technique is that the time-resolved of the thruster and the plasma is oscillatory, and that there is a physical relationship in Fourier space that ties the ion velocity distribution of the plasma to the discharge current oscillation of the thruster. Because the Fourier transform captures not only the amplitude but also the phase deviation from the sinusoidal basis function, the Fourier transfer function can capture the time-delay or phase difference between a variation in the input signal (discharge current) and the output signal (ExB probe measurement) due to the time of flight of ions or some other physical mechanisms. As mentioned in literature review, past research applied this Fourier analysis method for different experimental approaches to the Hall thruster exhaust and showed promising results.

5. *Maxwellian description*

When plasma is in a thermal equilibrium, the velocity distribution function of each charge-state of ions and electrons reach a distribution profile called the Maxwellian distribution, which takes the following form:

$$f_m(u) = n_0\sqrt{\frac{m}{2\pi kT}}\,exp\left(\frac{-m(u-u_0)^2}{2kT}\right)$$

While the Maxwellian description is not a complete description of the HET exhaust plasma, it is a oftentimes a good approximation. Mathematically, the expression can be simply written as:

$$f_m(u) = a\,exp(-b(u-u_0)^2)$$

where a, b, and u_0 are fit parameters.

The total ion density can be calculated as the infinite integral of the Maxwellian distribution function. Conveniently, it takes the following form:

$$\int_{-\infty}^{\infty} f_m(u)du = a\sqrt{\frac{\pi}{b}}$$

When multiple charge states are present in the plasma, each charge state often follows a different Maxwellian distribution. In these cases, the total ion velocity distribution function is simply described as the sum of two Maxwellian distributions. For example, for plasma consisting of singly and doubly charged ions, the distribution can be modeled by the following form:

$$f_{two\ peak}(u) = a_1\ exp\left(-b_1\left(u-u_{0,1}\right)^2\right) + a_2\ exp\left(-b_2\left(u-u_{0,2}\right)^2\right)$$

It is important to note that the ExB probe does not measure the ion velocity distribution function itself. However, because the ion current is equivalent to the product of ion flux and the charge of the ions in the population, the ExB probe measurement as a function of the filtering ion velocity is essentially a ion velocity distribution function where the height of each population is multiplied by the corresponding charge state.

III. Experimental Methodology

In this section, the experimental apparatus used for the experiment, including the Hall thruster and the diagnostics system, is described. An overview of the data analysis methods implemented in analyzing the raw measurements are also introduced.

1. Hall-Effect Thruster

The Hall-effect thruster (HET) used in this experiment is the ACME (Adaptive-field Central-cathode Magnetically-shielded Electric) thruster developed at the University of Washington SPACE Lab by Thoreau [12].The thruster is a magnetically-shielded Hall thruster

featuring electromagnets as the source of the magnetic field. While the notable design feature of the ACME thruster is the capability to easily vary the shape factor, namely the axial location of the inner magnetic pole, the thruster is operated with the conventional configuration throughout this experiment, in which the aft surfaces of the outer and inner magnetic poles align. The thruster has a mean channel diameter of 57 mm. Shown below is a picture of the thruster taken while it was in operation:

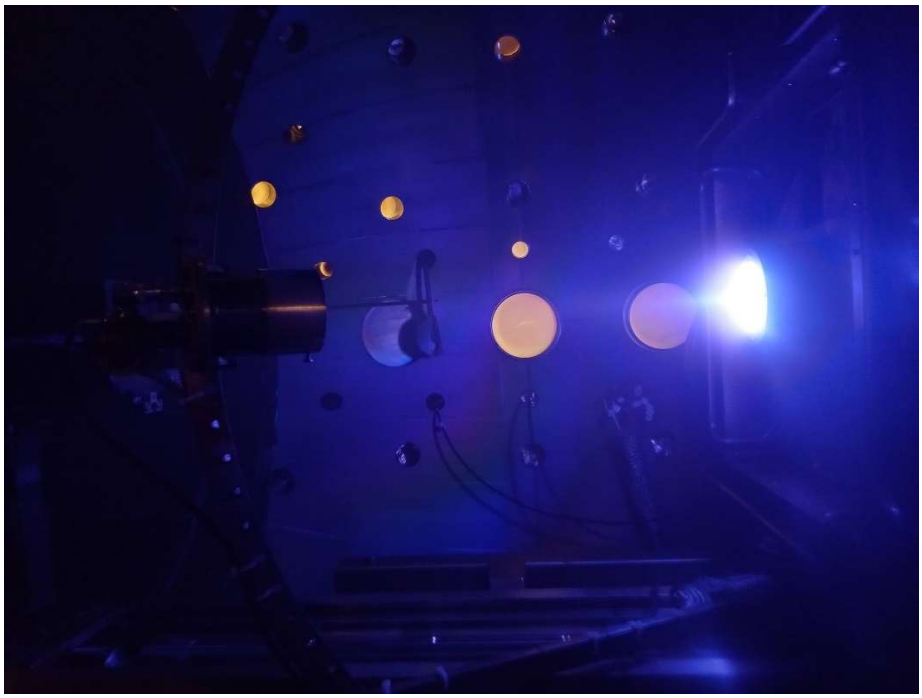

Figure III-1: The ACME thruster in operation.

Krypton is used as the propellant for this experiment. Krypton was chosen as the propellant because it is one of the common propellant choices for Hall thrusters, and the procurement cost is significantly cheaper when compared to xenon.

The thruster is operated inside the SPACE Lab Space Test Facility vacuum chamber under three operating conditions each of which corresponds to a different discharge voltage

(250V, 300V, and 350V). The nominal discharge current is kept constant at 1.87A for all three operating conditions. Small adjustments are made to other thruster parameters, such as thruster and cathode flow rates, as necessary in order to ensure reliable and operation of the thruster during testing.

The operating conditions of the thruster system tested in this investigation are summarized in Table III-1 below:

Table III-1: The operating conditions of the thruster system.

Trial Number	**Discharge Voltage (V)**	**Discharge Current (A)**	**Thruster Flow Rate (sccm)**	**Hollow Cathode Flow Rate (sccm)**
1	250	1.87	28.1	4.2
2	300		26.8	4.4
3	350		25.6	3.8

2. Diagnostics

The ExB probe used in this experiment was originally developed by Ha [10] at the University of Washington SPACE Lab for his master's thesis research. The thruster is aligned with the channel centerline of the thruster, at the distance of 89cm from the thruster front plane.

The exhaust ions enter the probe through a collimator with an orifice diameter of 1.75mm and the length of 63.5mm, thus effectively removing any ions with any nonnegligible nonaxial velocity. The perpendicular of magnetic field is applied by permanent magnets attached to the top and bottom plates of the probe. The average perpendicular magnetic field strength was

measured to be within the range between 0.110T and 0.129T. The average of the two limits is used as the representative value for this investigation. The electric field is applied by the two side plates, to which the bias voltage is applied. The separation between the electrodes is 3.81cm. The ion detector is made of tungsten. To prevent unwanted plasma-surface interactions, the front surface of the probe is protected by attaching graphite sheets. Shown below is the ExB probe setup inside the vacuum chamber:

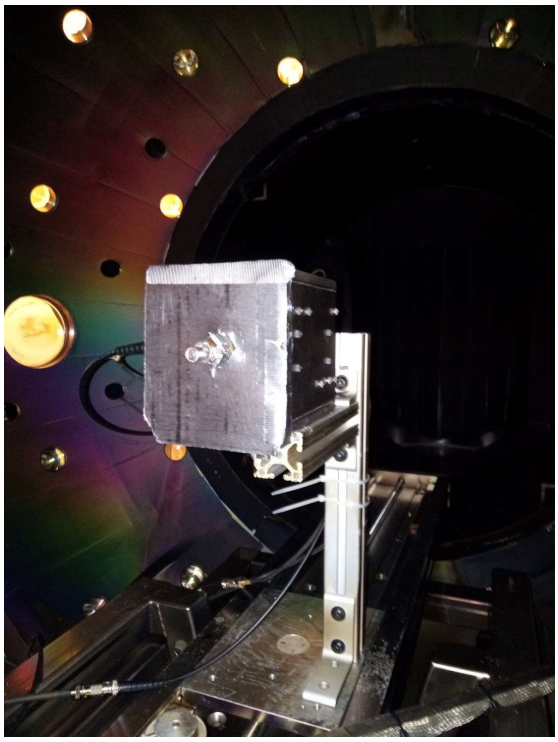

Figure III-2: ExB probe setup inside the vacuum chamber. The picture was taken before covering the probe with graphite sheets.

The bias voltage is supplied by the Kepco 500M high-voltage bipolar operational amplifier. To ensure that electric potentials are equal in magnitude but opposite in sign with relative to the ground are supplied to the two electrodes, resistors with equal resistance are placed between the output terminals and the ground. The amplifier amplifies the DC or slow-

varying voltage signal supplied to it by the factor of 50. The original signal is generated by FG-100DDS function generator for time-averaged and time-resolved measurements. The function generator is set to generate a triangular wave at the frequency of 1Hz, and the amplitude and DC offset are varied based on the ion velocity range of interest.

Simultaneously, the bias voltage supplied to the ExB probe by the bipolar operational amplifier is recorded by the oscilloscope as well. 10-x attenuation probes are used to convert the high-voltage signal to lower voltage suitable for measurement with the oscilloscope.

The ion current from the ExB probe is received by the Keithley 6485 Picoammeter, which converts small current to voltage at a high current-to-voltage ratio. The detection circuit is grounded to the chamber via the probe mount. The original plan was to use the Oriel Model 70710 pre-amplifier, which is a transimpedance amplifier with a bandwidth of up to 100kHz designed originally to amplify signals from photomultiplier tubes. However, the oscilloscope did not measure reasonable signal from the device and the decision to replace it with the picoammeter was made. The measurement of small, high-frequency (from the perspective of signal detection) signal from the probe is a major challenge in the design of time-resolved diagnostics with an ExB probe. Conventionally, picoammeters (e.g. Keithly 6485) are used to convert probe signal to voltage, but picoammeters have rise times too large to respond to the breathing mode oscillation. According to the manufacturer, Keithley 6485 Picoammeter has a rise time of 8ms for the analog output to rise from 10% to 90% in response to a step input at the settings used in this investigation. Modeling the analog input and output feature of the device as a LCR low-pass filter, the frequency response of the Keithley 6485 Picoammeter was approximated and visualized in the Bode plot below:

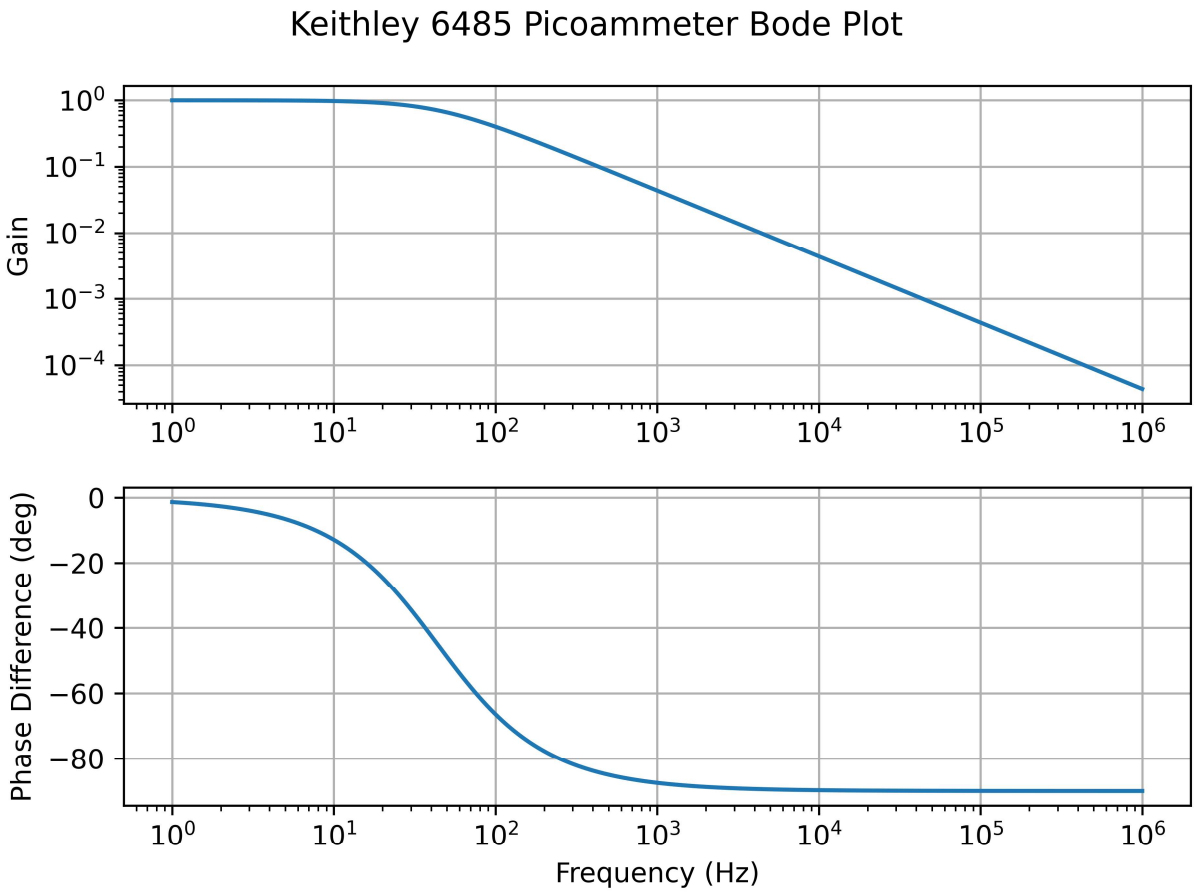

Figure III-3: The Bode plot describing the frequency response of the Keithley 6485 Picoammeter based on the published rise time.

From the Bode plot, it is estimated that the measurement is attenuated by a factor of 100~1000 for the range of frequencies of interest. To partially mitigate the significant attenuation of temporal variations expected in our measurements, the oscillatory behavior of the output signal is computationally amplified, as described in the next subsection.

The discharge current of the HET is measured by the B&K Precision CP6990 Current Probe, which is a current clamp capable of converting with high bandwidth both the AC and DC components of the current into voltage suitable for measurement with an oscilloscope. The gain

of the device is set at 0.1 V/A for the experiment. The current clamp does not directly interfere with the oscillating current, as the measurement of current is conducted through the induced magnetic field.

The two current signals, after converted to voltage by respective devices, are measured and recorded by the SDS2104X Plus oscilloscope. One million datapoints are recorded for the duration of 0.5 seconds, thus resulting in the measurement frequency of 2,000 kHz.

Shown below is a simplified schematic of the experimental setup:

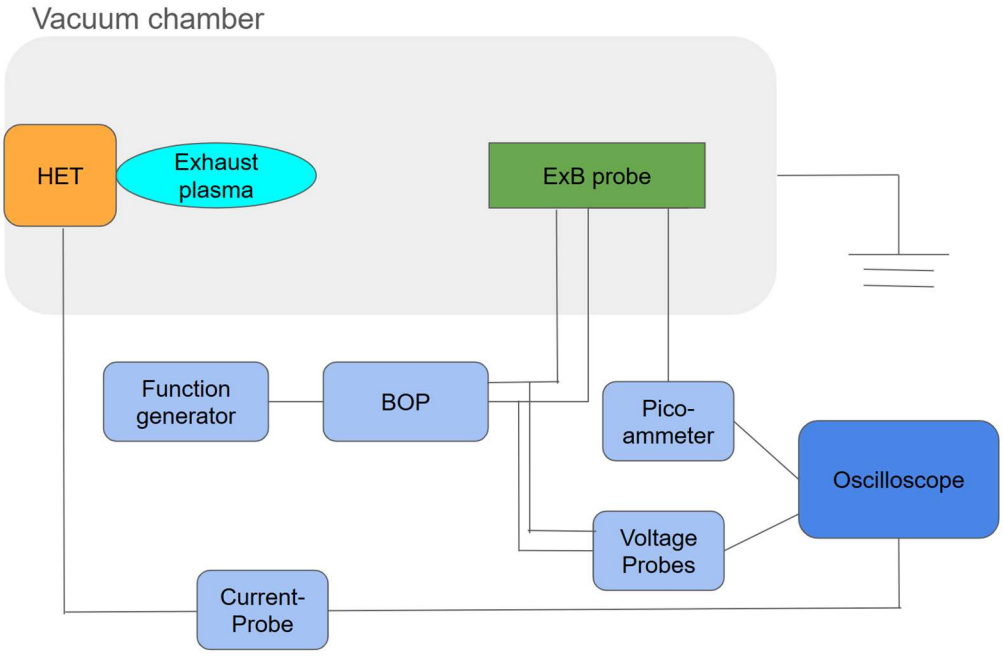

Figure III-4: A simplified drawing of the experimental setup.

3. Measurement Data Analysis and Algorithm

This subsection describes how a raw measurement dataset taken with the oscilloscope is processed through computer codes to obtain the time-resolved reconstruction of the synchronized ExB probe measurement. The computer codes are implemented in Python, and features a heavy

use of external packages including NumPy (for handling of multidimensional arrays and FFT analysis), SciPy (for numerical curve-fitting), Pandas (for the initial processing of raw measurement datasets), and Matplotlib (for visualization of outcomes).

After the raw CSV data file is loaded as a Pandas dataset, centered-rolling averaging with the window size of several datapoints is applied. The window size is varied based on the nature of oscillatory behavior. As later noted, the window size of 11 was used for the case of $V_d = 250$V, and the window size of 3 was used for the other two cases. Unit conversion is conducted, using known information of measurement devices.

Next, the dataset is split into an arbitrary number of subsets hereafter denoted as n_1, corresponding to the desired velocity resolution. The mean of the measured bias voltage within this subset is calculated and converted to the filtering ion velocity. The ion velocity is recorded and used as a label, as it becomes clear later. The n_1 parameter is set at 100 unless otherwise noted, resulting in the velocity resolution of 100 velocity divisions possible from the raw measurement.

The subset is then further divided into n_2 segments. The parameter n_2 needs to be adjusted manually for the algorithm to properly function for each operating condition, but the typical value is 10.

The discharge current and ExB probe signals, now divided into segments using two schemes, can be structured as three-dimensional arrays. The three axes correspond to ion velocity divided into n_1 steps, time, and division into n_2 segments. The first segment of discharge current measurement is separately saved to be used later as the sample signal.

Then, FFT can be applied to these three-dimensional arrays along the axis corresponding to time and yields another set of three-dimensional arrays, the axis originally corresponding to time now corresponding to frequency. This kind of axis-specific FFT operation can be easily implemented using NumPy's FFT package. The structure of and operation onto the three-dimensional array is described in the schematics below:

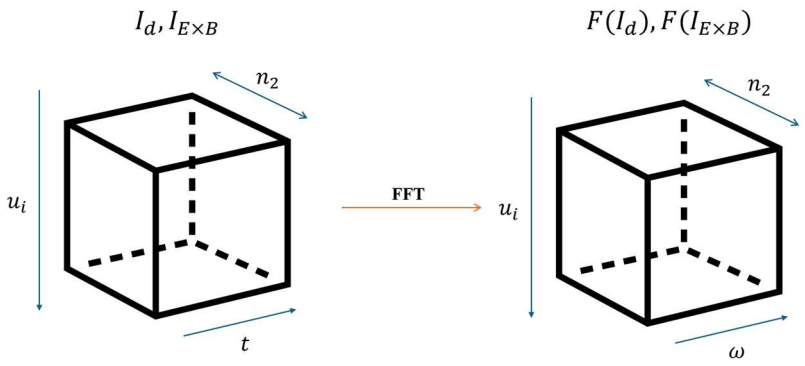

Figure III-5: Conceptual drawing of discharge current and ExB signal structured as 3D arrays and resulting Fourier transforms via FFT.

The transfer function between the Fourier transform of discharge current (input) and the Fourier transform of the ExB probe signal (output) can be formulated as an element-wise division between the two three-dimensional arrays, thus yielding the raw transfer function H_{raw} as another three-dimensional array with the same dimensionalities.

Axis-specific averaging is applied to the raw transfer function described as a three-dimensional array along the axis corresponding to subdivisions into n_2 segments. The averaging result in the averaged transfer function described as a two-dimensional array, axes of which correspond to ion velocity and frequency. Given n_2 parameter that is large enough, the averaging process theoretically mitigates random noise captured by the transfer function, as oscillatory

components not related causally two the two plasma parameters are expected to average to zero. This is an implementation of transfer function averaging used by Lobbia [5].

Various optional operations can be performed on the transfer function. Implemented in this investigation are frequency filters, base-measurement correction, and curve smoothing.

Frequency filtering (low-pass, high-pass, single-frequency) can be performed on the transfer function by setting components outside the range of interest to zero.

The ExB probe detects some ion current at settings where no ion flow is expected (e.g., at $V_p = 0\text{V}$). This is because of the presence of ions that travel through electromagnetic filtering and collide with the detector due to physical limitations of the probe, such as the collimator radius. This signal also oscillates corresponding to the oscillation in the discharge current, which influences the total ion flux. To elucidate the ExB probe signal comparable to the ion velocity distribution function, it is desirable that this signal is subtracted from the measurement. This is implemented by subtracting the average of rows (velocity axis) representing a region where no ion flux is expected to be detected for an ideal ExB probe from all rows of the transfer function.

To reduce irregularities and noise in the velocity space, rolling averaging is applied along the rows (velocity axis) of the transfer function. The window size used in this investigation is 5.

Lastly, each row of the two-dimensional transfer function is multiplied by the Fourier transform of the sample discharge current signal. The multiplication between rows here is elementwise. The product is also a two-dimensional array. Applying inverse FFT to this two-dimensional along the axis corresponding to frequencies, a reconstructed ExB probe measurements as a function of time synchronized to the sample discharge current is obtained as a two-dimensional array, axes of which correspond to ion velocity and time.

4. Mitigation of Signal Attenuation

The previous subsection provided the description of an algorithm necessary to obtain the reconstructed ExB probe measurement as seen by the oscilloscope. However, as noted in the explanation of the experimental setup, it is expected that there is a significant attenuation between the ion current signal and the analog output from the Keithley 6485 Picoammeter. From the Bode plot, the factor of attenuation for the frequency range of interest is estimated to be in the order of 100~1,000, but applying amplification around this order would result in nonphysical representation of the data due to amplified noise. For this reason, a conservative amplification by the factor of 10 for oscillatory deviation from the time-averaged measurement is used in this investigation, unless otherwise noted.

The amplification is not a complete correction for the signal attenuation, but it is expected that it brings the data closer to the physical behavior.

The amplification is implemented by at each time step, first calculating the deviation from the time-averaged measurement, and then adding the multiplied deviation to the time-averaged measurement.

5. Curve-fitting analysis

Curve-fitting analysis is conducted on the amplified result of the reconstructed ExB probe measurements, unless otherwise noted, with the two-peak Maxwellian distribution function. Python's external package SciPy is used for implementing the numerical curve fitting. The six parameters obtained at each time step (three for singly charged ions, and three for doubly charged ions) are then used to calculate the ion current from each charge state by evaluating the

algebraic expression for the infinite integral. The obtained ion currents are then compared with each other to obtain the fraction of singly charged ions.

IV. Results & Discussion

The results obtained from analyzing experimental data are discussed. First, the summary of time-averaged analysis is provided to serve as the baseline for understanding the time-resolved results. Then the section discusses the time-resolved data. Implications of the results are mentioned.

The pressure of the vacuum chamber without the thruster operating was measured to be 1.9×10^{-6} Torr. The background gas was assumed to be at room temperature, at 293K.

1. Time-Averaged Analysis

For each operating condition, the signal collected from the ExB probe is analyzed as time-averaged data. After accounting for noise and oscillatory behavior in the signal by computing the average for each small increment of bias voltage, and converting the bias voltage

values to corresponding ion speeds, we obtain the results plotted below:

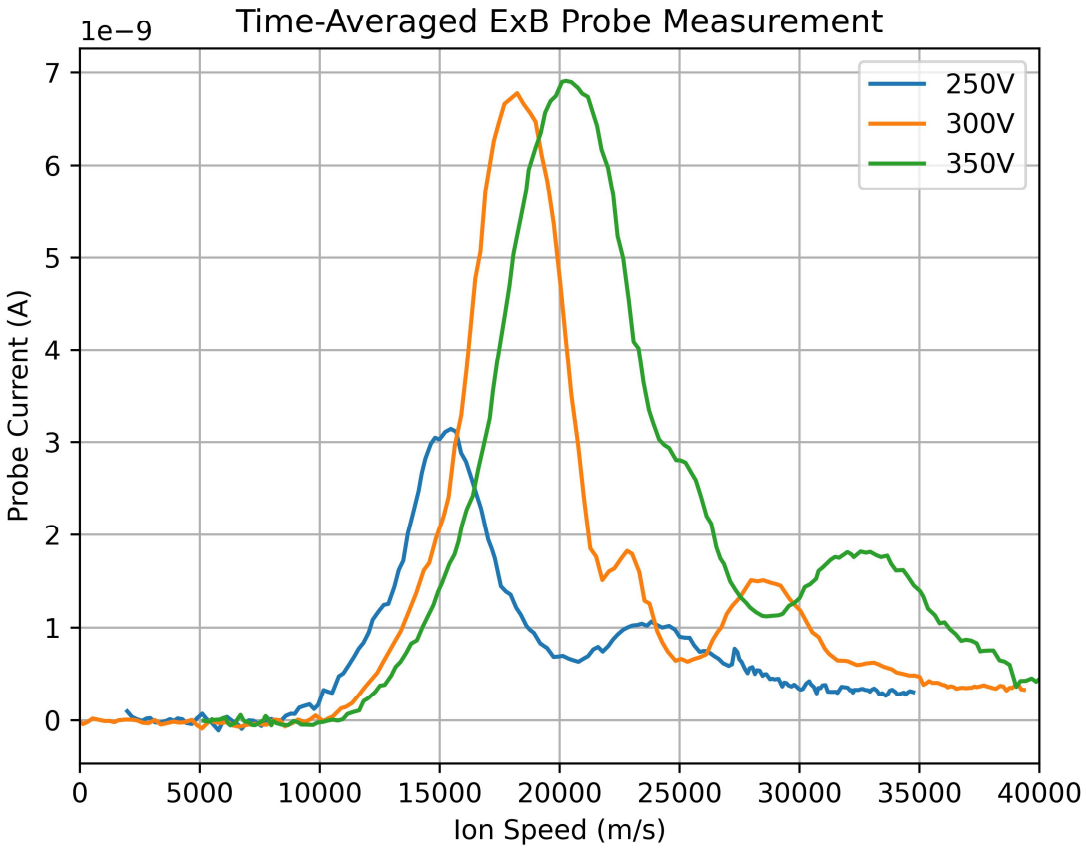

Figure IV-1: Time-averaged ExB probe measurement at three operating conditions.

The plots show that in each of the three operating conditions, the ion velocity distribution function approximately exhibited bimodal Maxwellian distribution, the larger peak and the secondary peak likely corresponding to singly and doubly charged ions, respectively. The peak velocities of the two peaks increased as the cathode-to-ground voltage increased. The variation in the peak heights or the area under the curve is likely explicable by some variation in the ionization efficiency of at each operating conditions, while more investigation is needed to make a determinative conclusion on the cause of the variation. It is worth noting that the variation in

propellant flow rate likely does not explain the variation in peak heights or area under the curve, based on the specific operating conditions.

The two-fluid Maxwellian distribution profile was numerically fitted onto the real measurement plotted above for each operating condition. The results of numerical fitting are plotted below

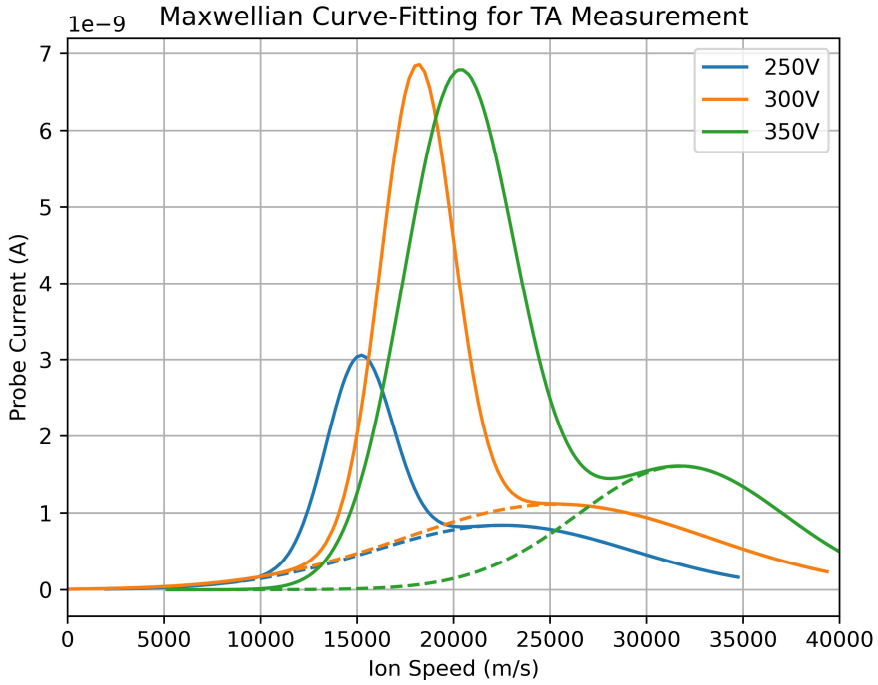

Figure IV-2: Numerical curve-fitting with two-fluid Maxwellian distribution profiles. Dotted curves plot the distribution profile of the secondary peak (doubly charged ions).

Based on the best-fitting parameters, the size of the ion current corresponding to each charge state was computed for each operating condition. Furthermore, the charge-exchange correction model was applied for each operating condition to approximate the charge-state distribution at the thruster exit plane. For both the uncorrected and the corrected values, the fraction of ion current due to the singly-charged ions over the total ion current were plotted against the discharge voltage in the plots below:

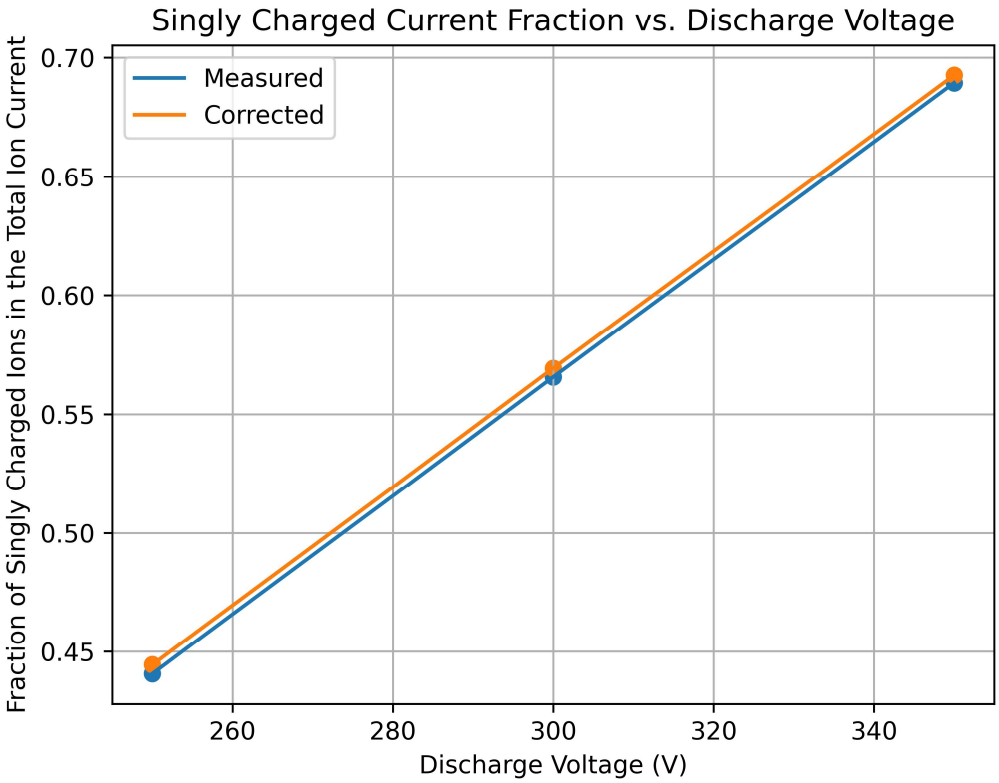

Figure IV-3: The variation of charge state fraction against discharge voltage.

One can observe that the fraction of singly charged ions in the total ion current increased linearly as the discharge voltage was increased. The CEX correction model only resulted in a slight increase in the fraction of singly charged ions in the total ion current. Although the effect of CEX was small in this specific experimental setup, it is worth noting that charge exchanges could easily have a nonnegligible effect on the measurement depending on the experimental setup.

2. *Time-Resolved Analysis*

First, the discharge current measurement after applying the moving-averaging with the step size of 3 is plotted for each operating condition. The results are plotted in Figure IV-4 below:

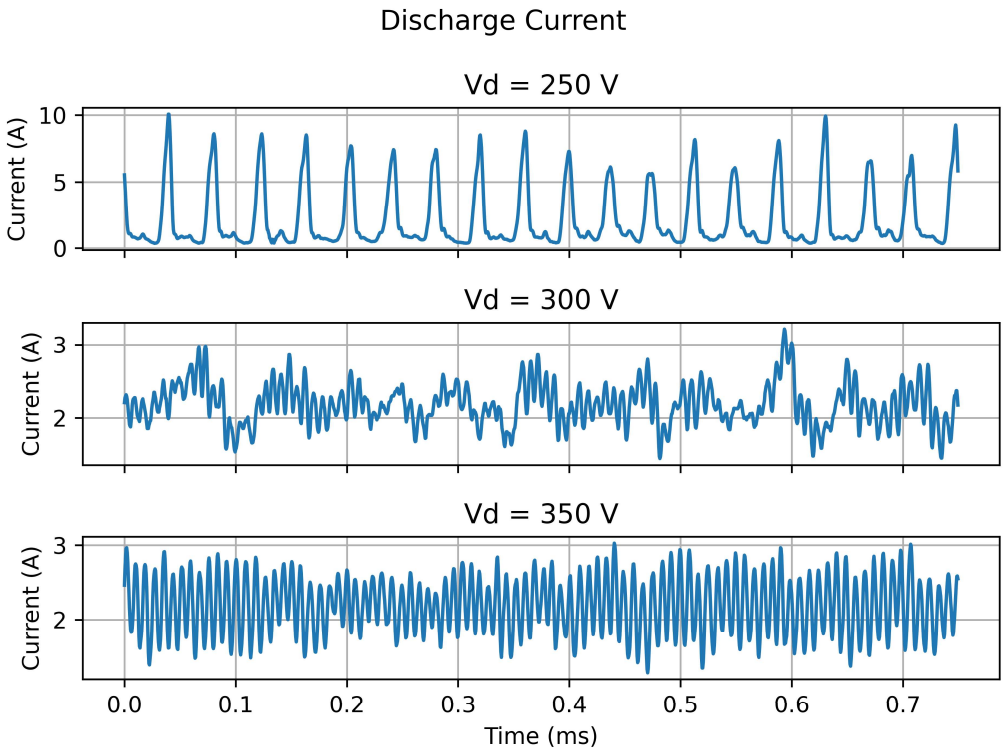

Figure IV-4: Measurement of discharge current at three operating conditions.

It is observed that at the discharge voltage of 250V, the thruster exhibited a higher amplitude of oscillation than at the discharge voltage of 300V or 350V. At the discharge voltage of 250V, the breathing-mode oscillation was the overwhelming dominant mode of oscillatory behavior. At 300V, while the dominant oscillation mode remains to be the breathing-mode oscillation, which had a lower frequency compared to the operation at 250V, there is an increase in the presence of higher-frequency components. At 350V, the higher-frequency oscillatory modes become the dominant oscillation mode, resulting in a nearly sinusoidal oscillation at high frequency. Table

below lists the most dominant frequency at each operating condition obtained based on Fourier analysis of the discharge current:

Table IV-1: Base frequency of discharge current oscillation

Discharge Voltage	250 V	300 V	350V
Frequency	25.5 kHz	15.5 kHz	120.5 kHz

Synchronization of the ExB signal was performed at each operating condition. The parameters of the reconstruction algorithm were manually adjusted for each operating condition to obtain representative data. The results are summarized below.

(i) $\boldsymbol{V_d = 250V}$

In the case of $V_d = 250$V, the oscillatory behavior of the discharge current was dominated by the low-frequency oscillation around 25kHz. This frequency is consistent with the typical range of breathing-mode oscillations. For this reason, the analysis was conducted purely for the most dominant frequency of the discharge current. n_1 and n_2 parameters for the algorithm were set to 100 and 50, respectively.

First, the Fourier transfer function at this specific frequency is plotted below as a function of ion velocity together with the time-average ion velocity distribution function:

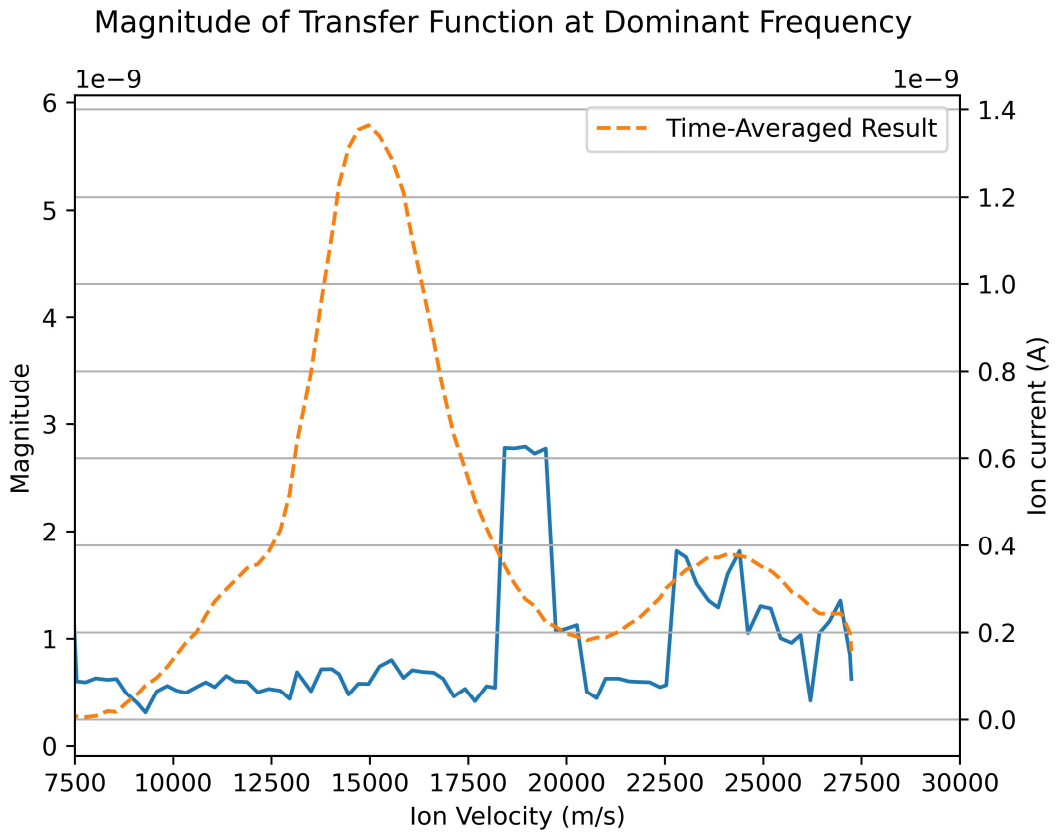

Figure IV-5: Fourier Transfer function at V_d=250V

Since the transfer function was plotted for a specific frequency, the transfer function essentially describes the amplitude of oscillation at a given fixed frequency as a function of the ion velocity. It is observed that the magnitude of the transfer function is particularly high throughout the velocity domain corresponding to the secondary peak (doubly charged ions). On the other hand, the result implies that the primary peak (singly charged ions) does not show any notable correspondence to the oscillation of the discharge current at this frequency. It is worth noting that there is another velocity range with particularly high magnitude of transfer function, between the two peaks. This region corresponds to the region in which some irregularity in the

time-averaged ion velocity distribution function was consistently observed for all three operating conditions, including $V_d = 250\text{V}$.

The obtained transfer function was then used for the synchronization of ExB probe measurements. The resulting ExB probe signal as a function of ion velocity and time is plotted below. The modified result in which the deviation from the time-averaged result is amplified by the factor of 10 is also plotted.

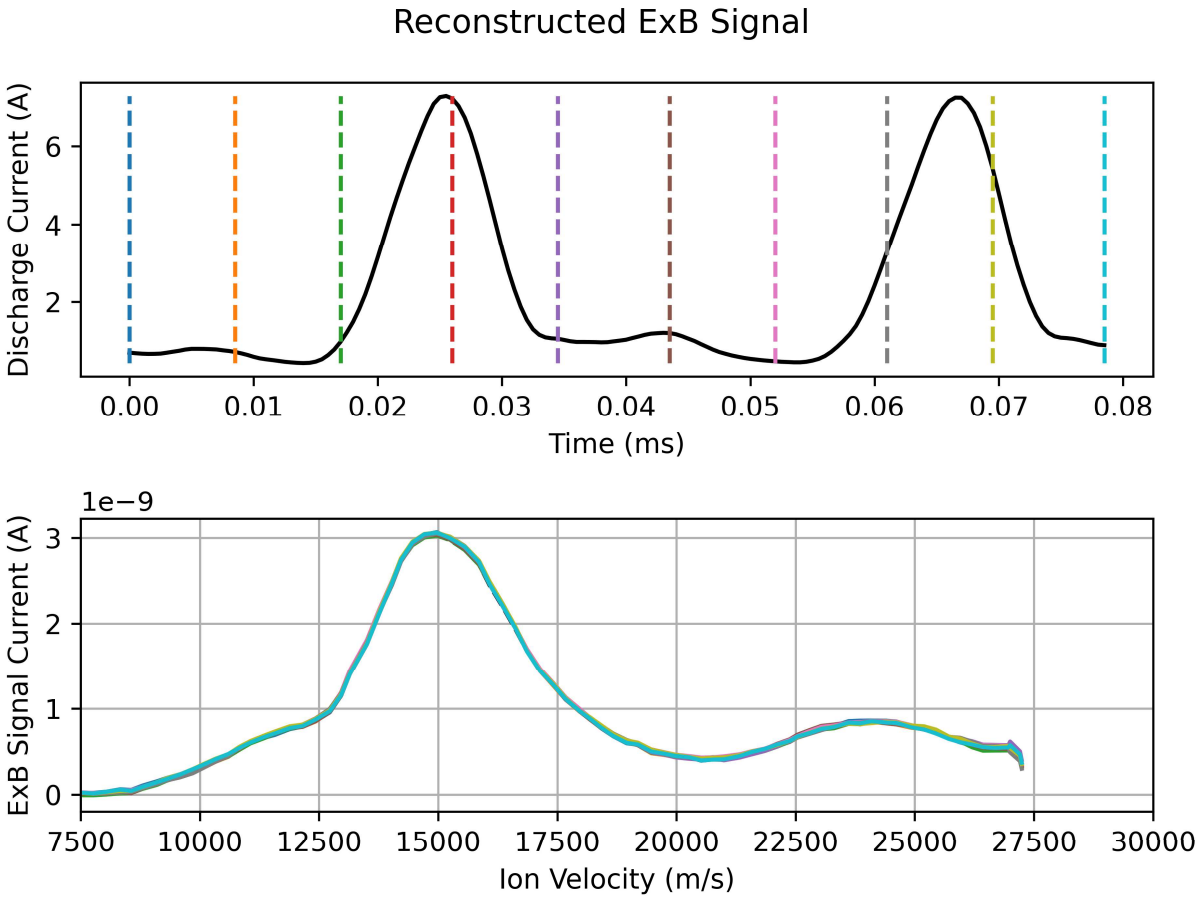

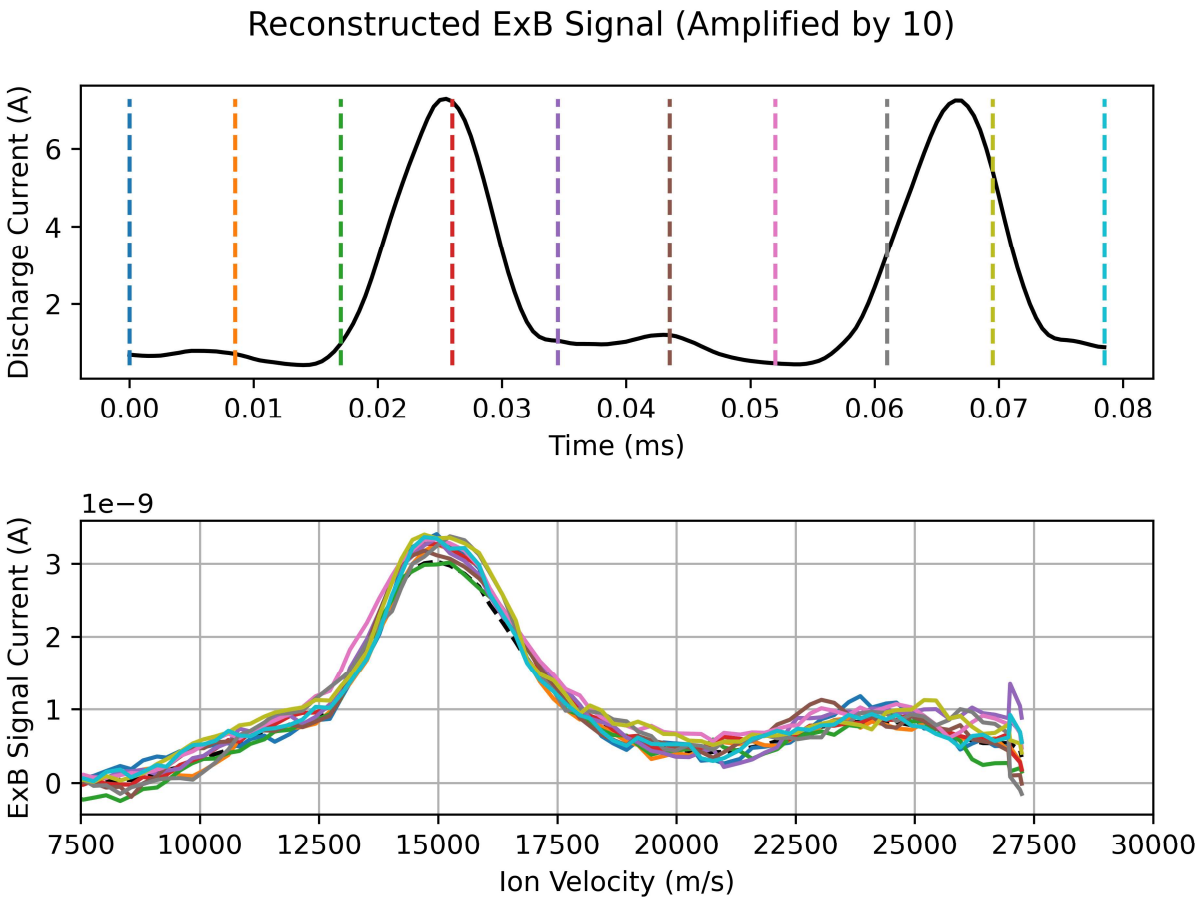

Figure IV-6: Unamplified (top) and amplified (bottom) ExB probe measurements at $V_d = 250$V.

The amplified result was also plotted as a contour plot:

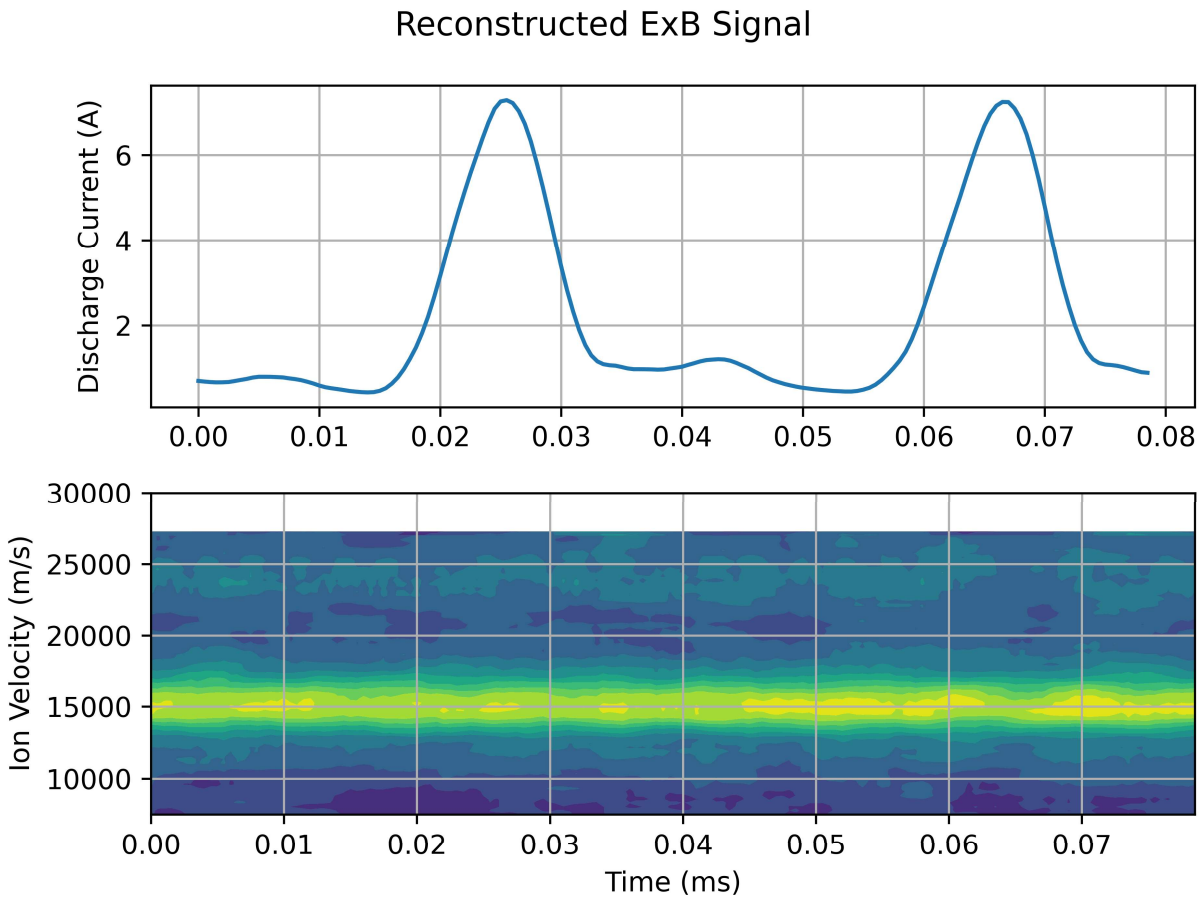

Figure IV-7: The amplified ExB measurement plotted as a contour plot.

The amplitude of oscillation is generally small, but the amplitude of oscillation for the secondary peak (doubly charged ions) in comparison to its peak height was greater than that of singly charged ions.

Curve-fitting with the two-peak Maxwellian profile was conducted onto the amplified reconstructed signal and generally led to reasonable outcomes. The result of curve fitting is plotted below together with the time-averaged signal:

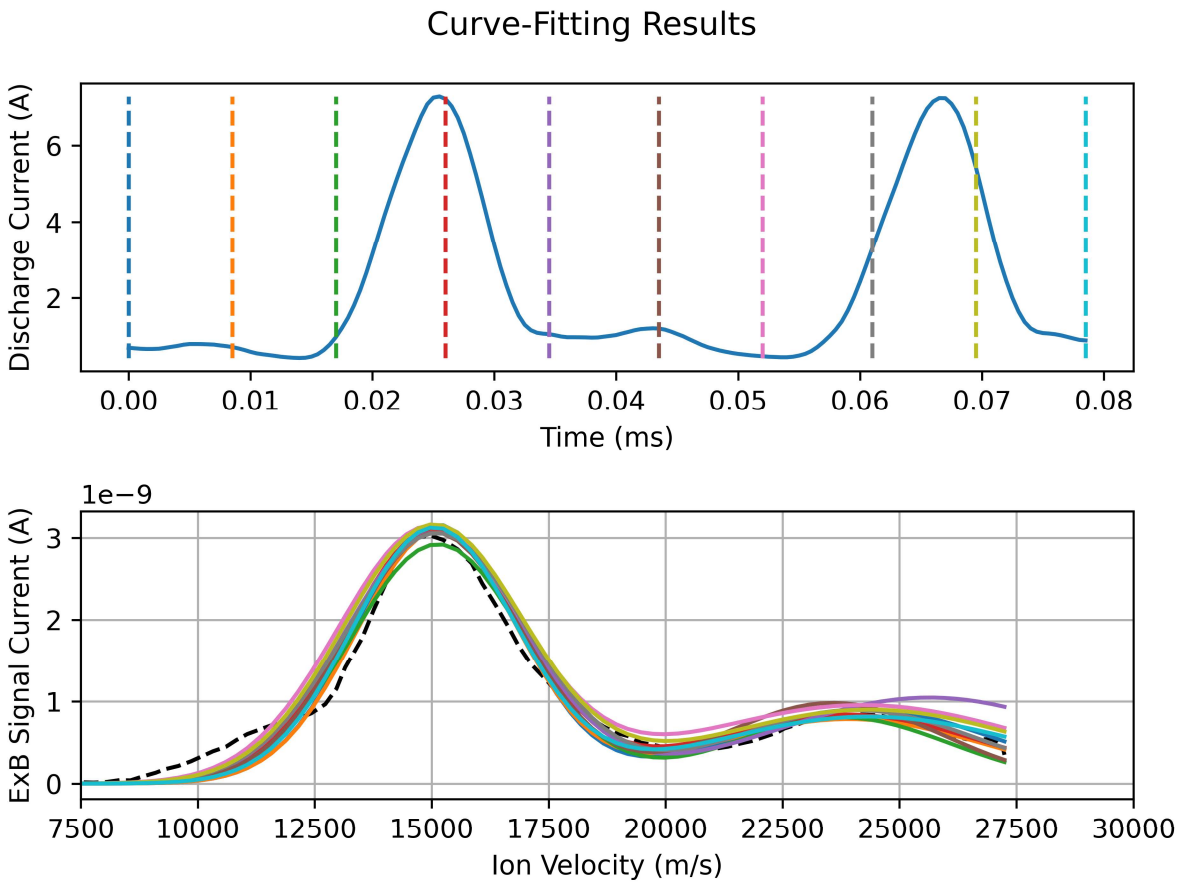

Figure IV-8: Curve-fitting results for the amplified synchronized ExB measurement at V_d=250V

The best-fitting parameters obtained at each time step are then used to analyze the charge-state characteristics. The results are plotted below:

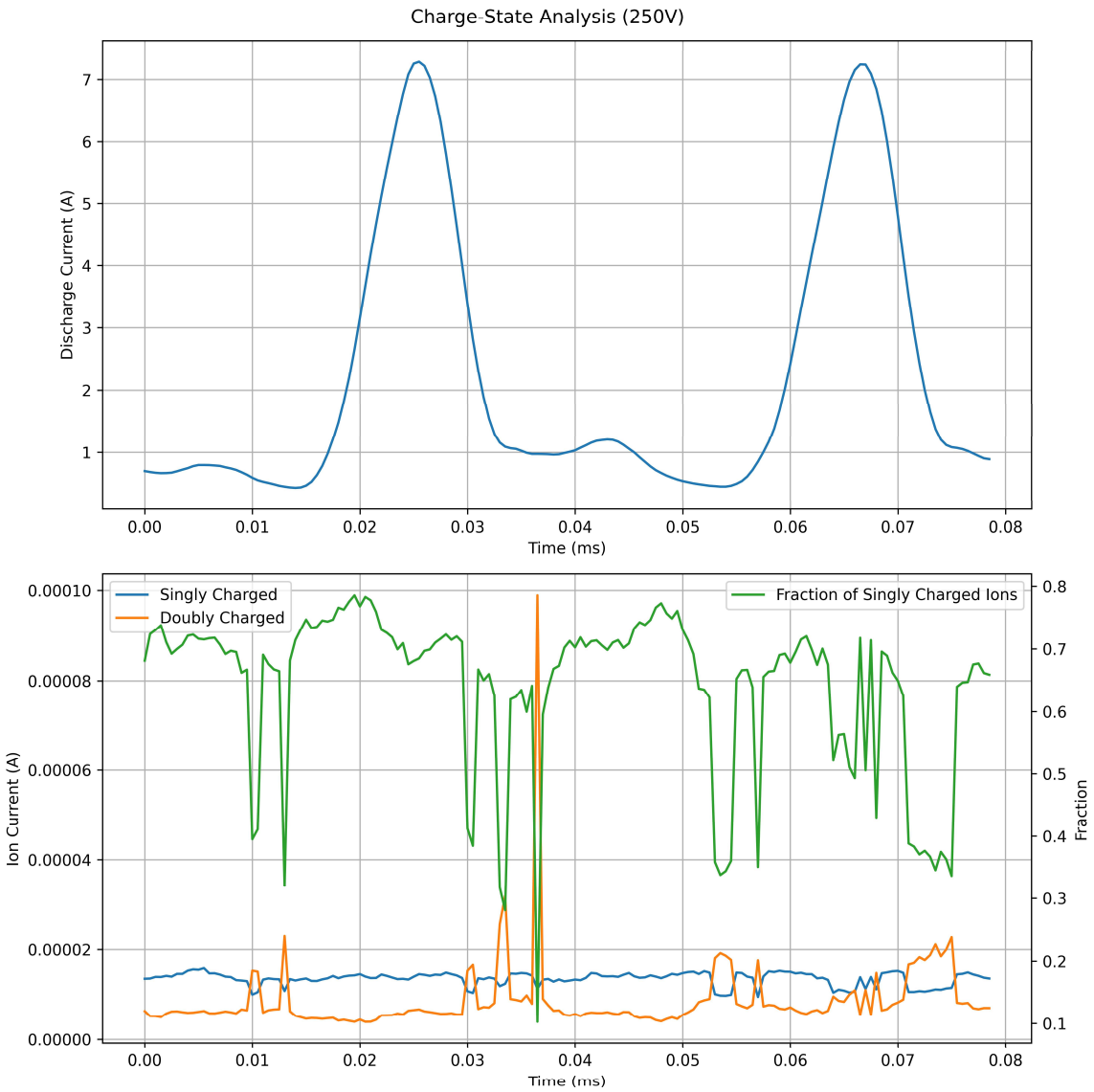

Figure IV-9: Results of charge-state analysis based on the best-fitting parameters.

It can be observed that the ion current due to doubly charged ions shows much higher oscillation amplitude compared to the singly charged ions. This results in large oscillation in the charge-state distribution of plasma. While it is worth noting that the analysis is based on amplified signals, the fraction of singly charged ions in the total ion current oscillates at the frequency close to 40%.

(ii) $\boldsymbol{V_d = 300V}$

From the discharge current measurement, it is observed that the oscillatory behavior at the discharge voltage of 300V includes oscillations at multiple frequencies with approximately equal amplitudes. For this reason, the single-frequency filter was not applied, and instead low-pass filtering with the cutoff frequency of 200kHz was applied. The n_1 parameter was kept at 100, but the n_2 parameter was set to 5.

The resulting Fourier transfer function was visualized as a function of velocity together with the time-averaged distribution function for the frequency corresponding to the maximum value of the transfer function at each velocity. The result is plotted below:

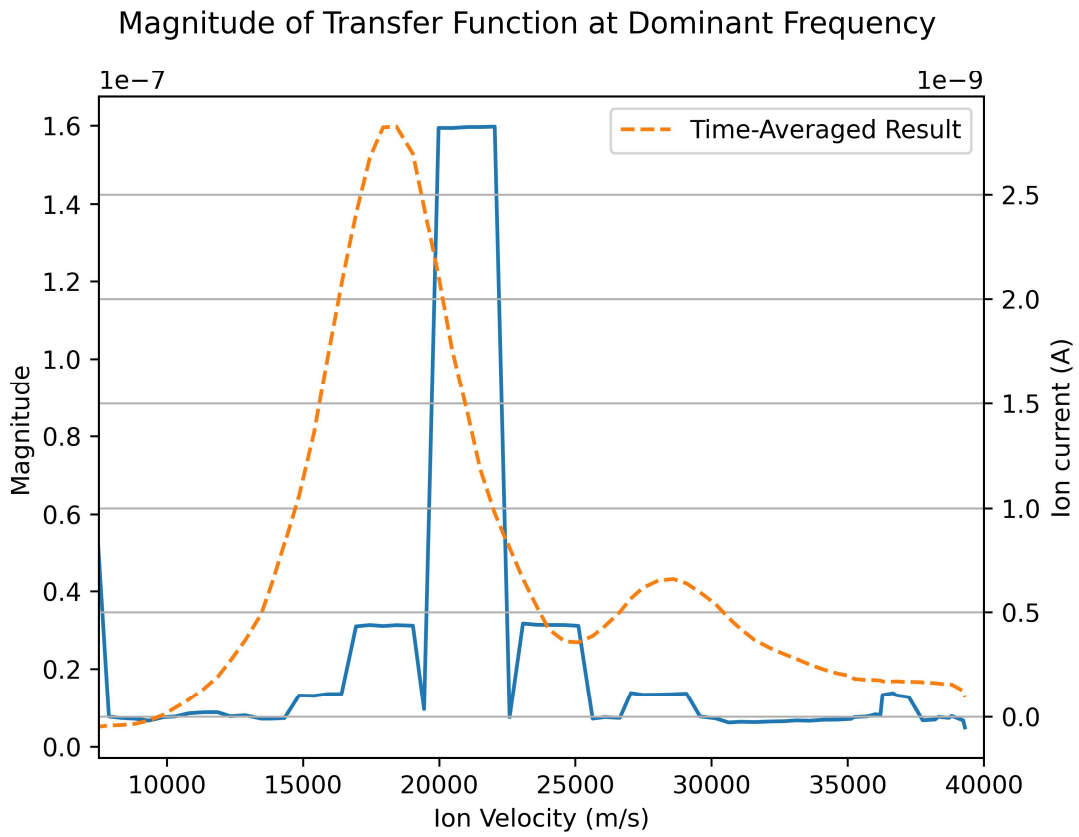

Figure IV-10: Maximum of the Fourier transfer function as a function of ion velocity at $V_d = 300V$.

One can observe that while there is relatively high correspondence between the discharge current and the primary and secondary peaks, the most notable correspondence is with the right shoulder of the primary peak. It is worth noting that this region corresponds to the velocity range where some presence of non-Maxwellian singly- or doubly- charged ions is suspected.

While the transfer function does not follow a physically intuitive pattern, the synchronization of the ExB probe measurements was attempted following the algorithm. The obtained result, as well as the result where the deviation from the time-averaged result is amplified by the factor of 5, is plotted below:

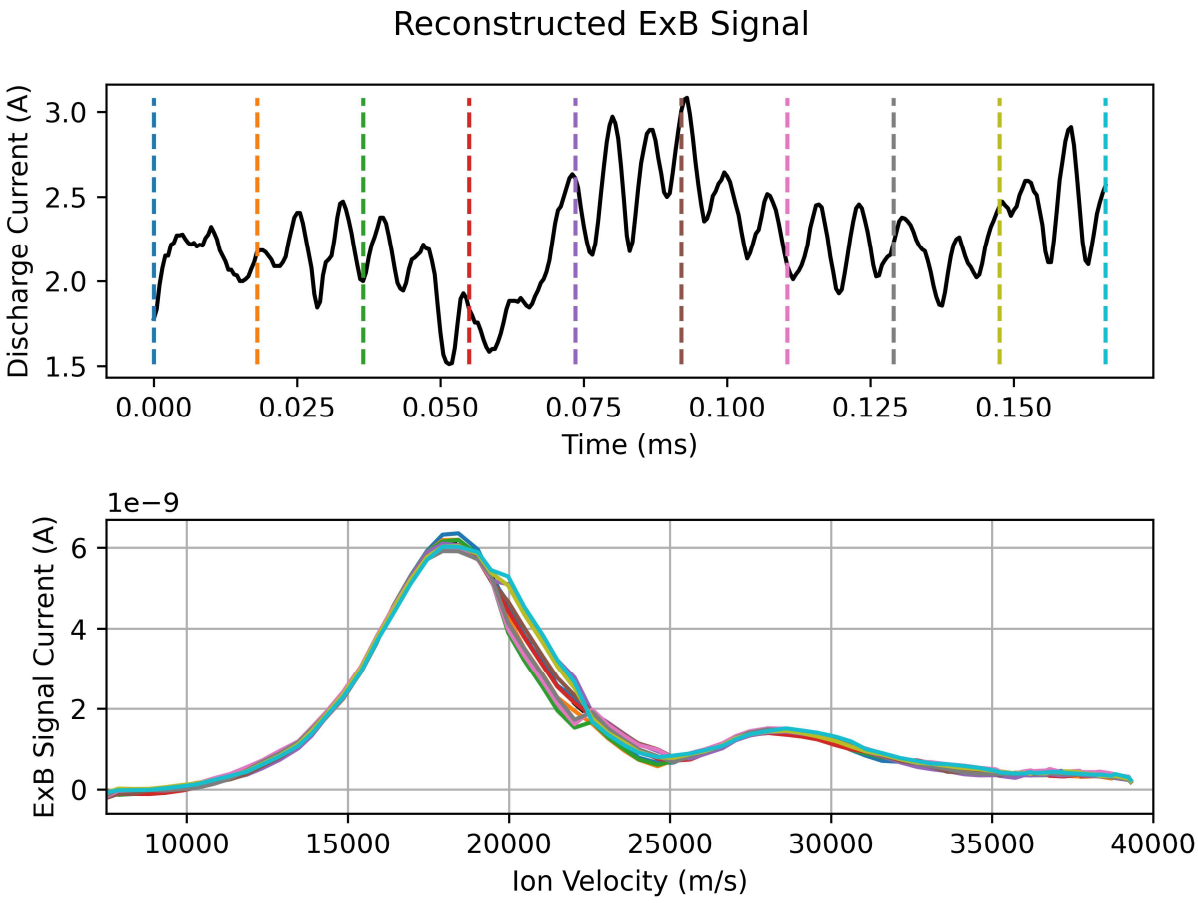

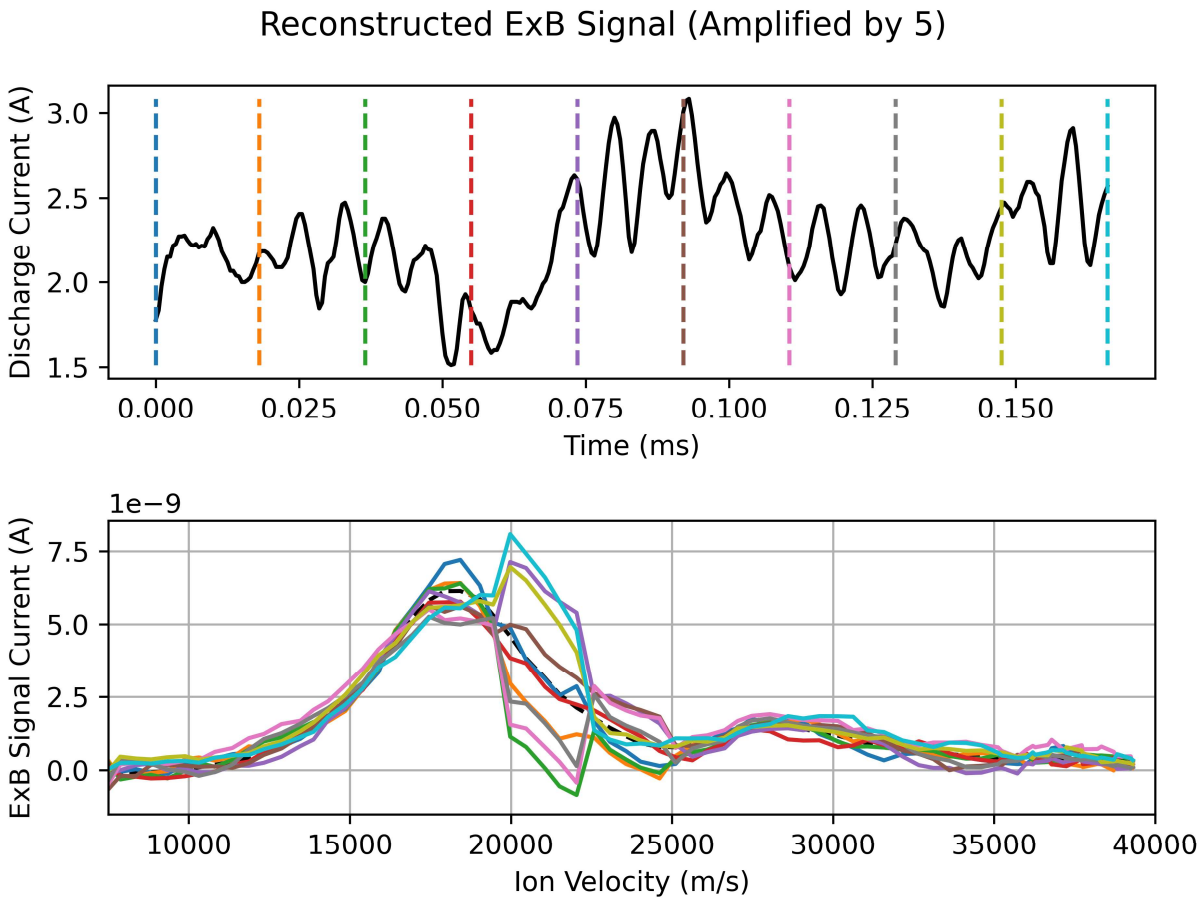

Figure IV-11: Visualization of unamplified (top) and amplified (bottom) temporal variation of the reconstructed time-resolved ExB measurement at V_d=300 (V)

One can observe that the right shoulder of the primary peak experiences high-amplitude oscillation. While the reconstructed time-resolved ion velocity distribution function does not capture the full nature of the oscillatory behavior in this velocity domain, the suspected presence of irregular phenomenon in this domain agrees with the time-averaged measurement.

The amplified synchronized measurement was also visualized as a contour plot below:

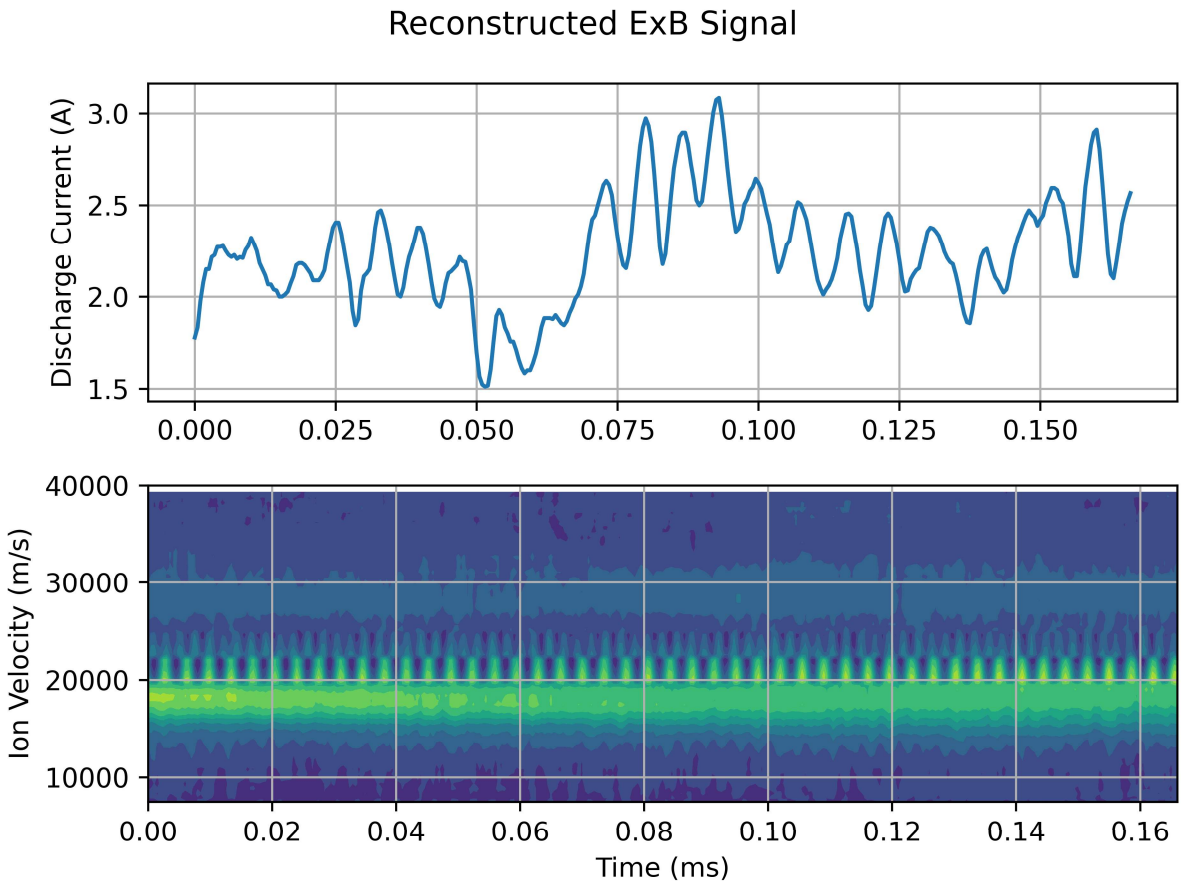

Figure IV-12: Amplified reconstructed ExB probe measurement at $V_d = 300\text{V}$ visualized as a contour plot.

One can observe that the high-amplitude oscillation of the "shoulder" region occurs in correspondence to higher-frequency oscillation of the discharge current around approximately 120kHz. The primary and secondary peaks weakly oscillate in height in correspondence to the same high-frequency oscillations. It is also observed that the height of the primary peak corresponds to the low-frequency variation of the discharge current.

While curve-fitting with the two-peak Maxwellian distribution function was attempted for the amplified reconstructed signal, it largely failed leading to non-physical results. The failure is largely explicable by the aforementioned presence of high-amplitude irregularity.

(iii) $\boldsymbol{V_d = 350V}$

Since the oscillatory behavior observed in the discharge current measurement was dominated by high frequency oscillation around 120kHz for the discharge voltage of 350V, the n_2 parameter was increased to 10 while the parameter n_1 was kept at 100.

Following the algorithm described in the previous chapter, the Fourier transfer function was obtained. The figure below shows the magnitude of the transfer function between the discharge current and the ExB probe signal at the dominant frequency of the discharge current, as a function of ion velocity:

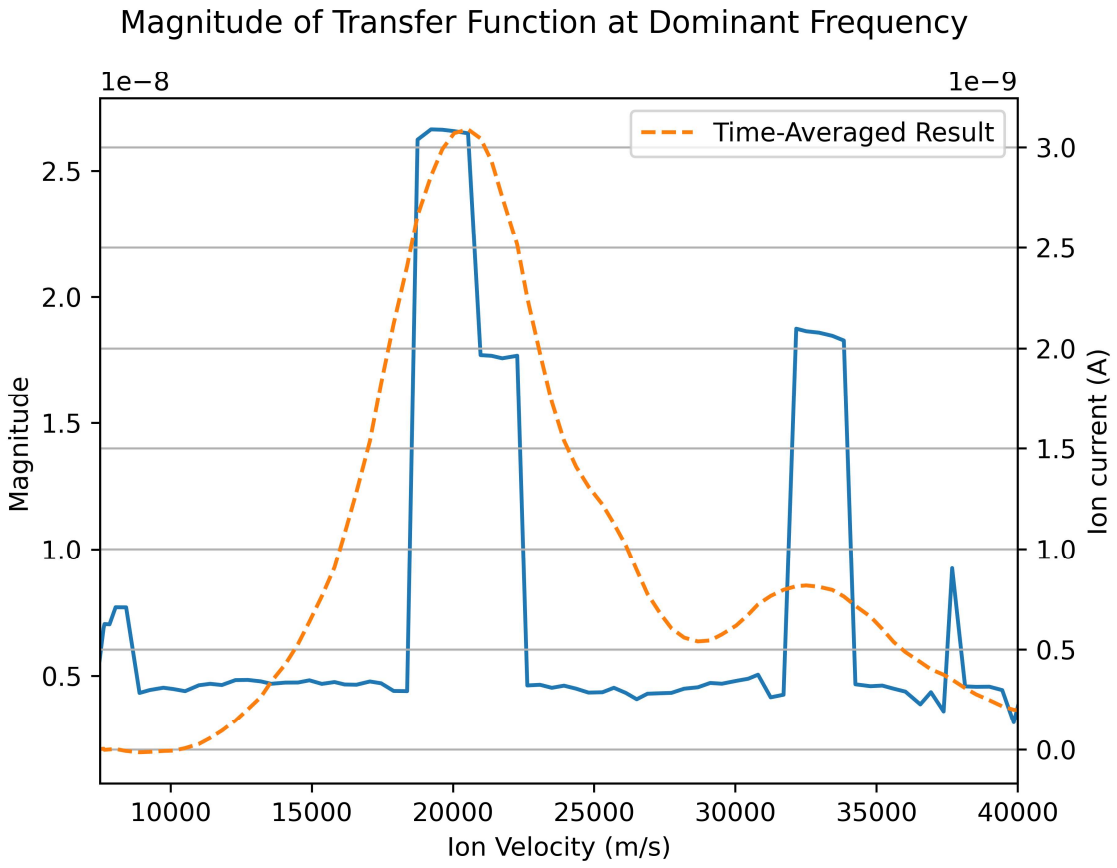

Figure IV-13: The magnitude of the Fourier transfer function (blue solid line) plotted together with the time-averaged ExB probe signal (orange dotted line), as a function of the ion velocity.

Since the transfer function was plotted for a specific frequency, the transfer function essentially describes the amplitude of oscillation at a given fixed frequency as a function of the ion velocity. The visualized transfer function shows that the correspondence between the discharge current oscillation and the oscillatory behavior of the ion velocity distribution function is highly selective based on the velocity. Oscillation at the discharge frequency is strong only in velocity domains close to the two peak velocities of the time-averaged ion velocity distribution function. Physically, this result implies that the oscillatory behavior of the thruster propagates relatively strongly to the ions accelerated closer to the group velocities of respective populations, and less strongly to ions accelerated to velocity ranges outside the peaks.

One can also observe that while the oscillation amplitude around the secondary peak (doubly charged ions) was smaller than around the primary peak (singly charged ions), the oscillation amplitude secondary peak in relative to height of the distribution peak was larger than the oscillation amplitude of the primary peak in relative to the height of the primary peak. This implies that the oscillatory behavior of the distribution profile of doubly charged ions (e.g., ion flux, group velocity, ion temperature etc.) is driven more strongly than the singly charged ions are at this frequency. This phenomenon could be explicable by the hypothesis that the oscillatory behavior of the thruster propagates to the generation mechanism of secondary charged ions, because the distribution profile of the secondary charged ions are affected not only by the fundamental acceleration mechanism (which affects all ions) but also by the generation mechanisms.

The synchronization of the ExB probe measurements showed reasonable results, resulting in a measurement of oscillatory behavior of the ion velocity distribution profile around the time-resolved measurement. Plotted below are the results of the signal synchronization at several

selected time steps. In the second plot, the deviation from the time-averaged distribution was amplified by the factor of 10 to elucidate the temporal variation of the ion velocity distribution function.

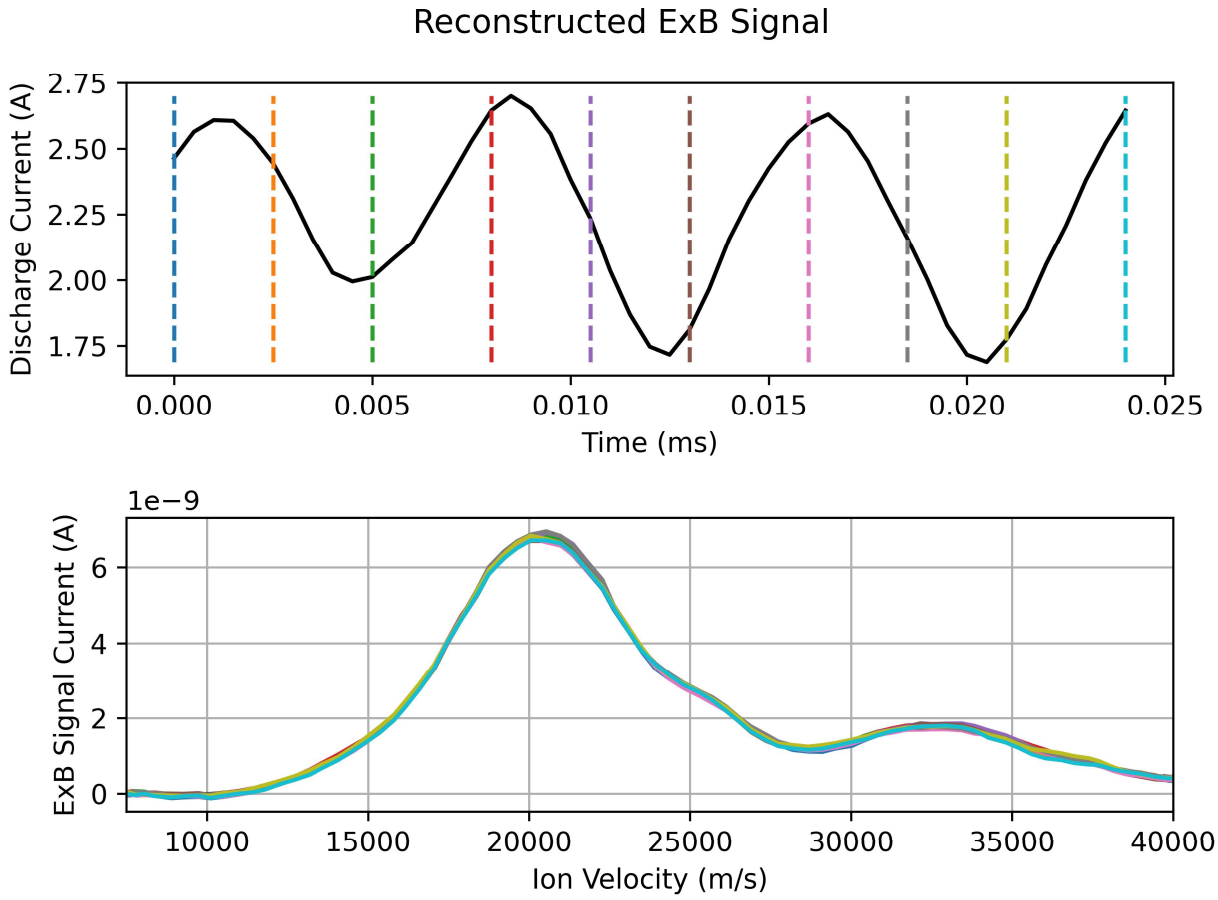

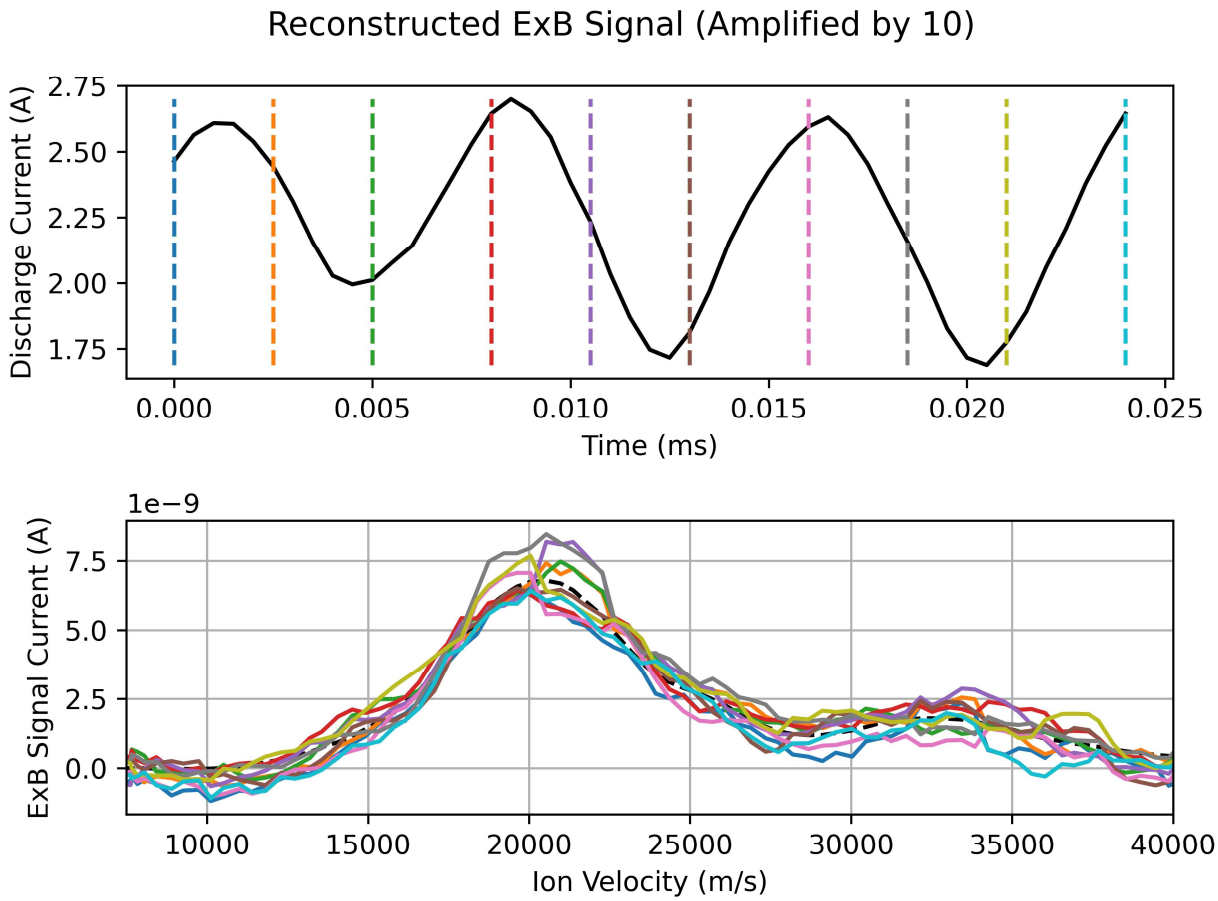

Figure IV-14: Visualization of unamplified (top) and amplified (bottom) temporal variation of the reconstructed time-resolved ExB measurement at $V_d = 350$ (V)

The amplified reconstructed signal was also visualized as the color plot below:

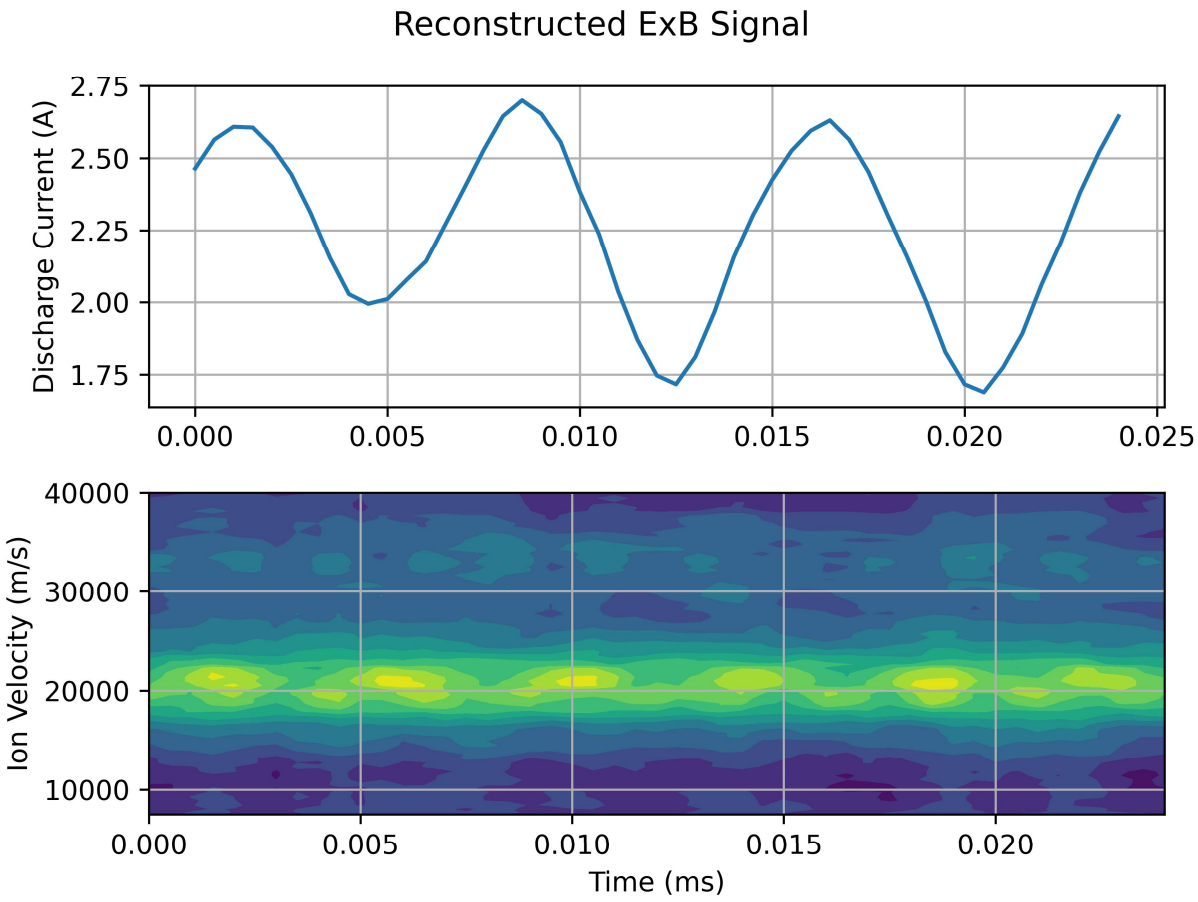

Figure IV-15: Contour plot for the amplified reconstructed ExB signal at 350V.

From the contour plot of the amplified result, one can observe that the primary peak (singly charged ions) exhibit oscillatory behavior both in its height and in its group velocity. Additionally, from the line plot, one can observe that the velocity distribution profile remains below the time-averaged profile around the primary peak for most of the time steps, but exhibits profiles significantly higher than the time-averaged profiles in a few selected time steps. This implies the presence of sporadic, short yet strong “bursts” of singly charged ions.

The behavior of the secondary peak (doubly charged ions) is less clear from the plots, but the distribution profile generally oscillates evenly in height around the time-averaged profile.

The oscillation is not necessarily in-phase with the primary peak, while it is worth noting that the singly charged ions and doubly charged ions experience different time delay between the thruster and the probe due to the difference in speed. As noted in the analysis of the transfer function, the oscillation amplitude of the secondary peak in relative to the height of the time-averaged peak is larger in comparison to the primary peak.

Parametric curve-fitting was applied to the reconstructed signal amplified by the factor of 10 with the two-peak Maxwellian distribution function. The curve-fitting was successful at each time step and resulted in successfully capturing the oscillatory behavior of the distribution function. The result is plotted in the line plot below:

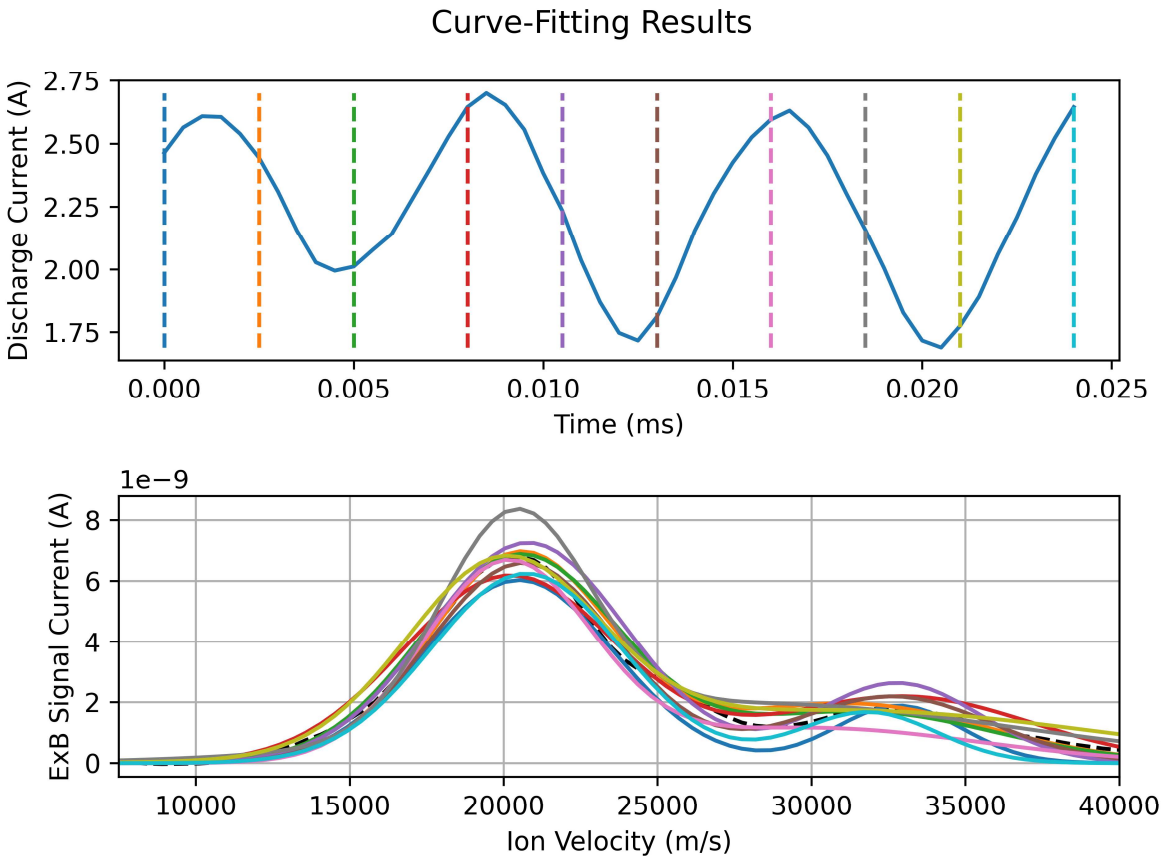

Figure IV-16: Visualization of curve-fitting results with the two-peak Maxwellian profile.

The two-peak Maxwellian profile captures the measures velocity distribution function well at each time step.

Finally, the best-fitting parameters at each time step obtained from curve-fitting were used to analyze the charge-state distribution. The results are plotted below:

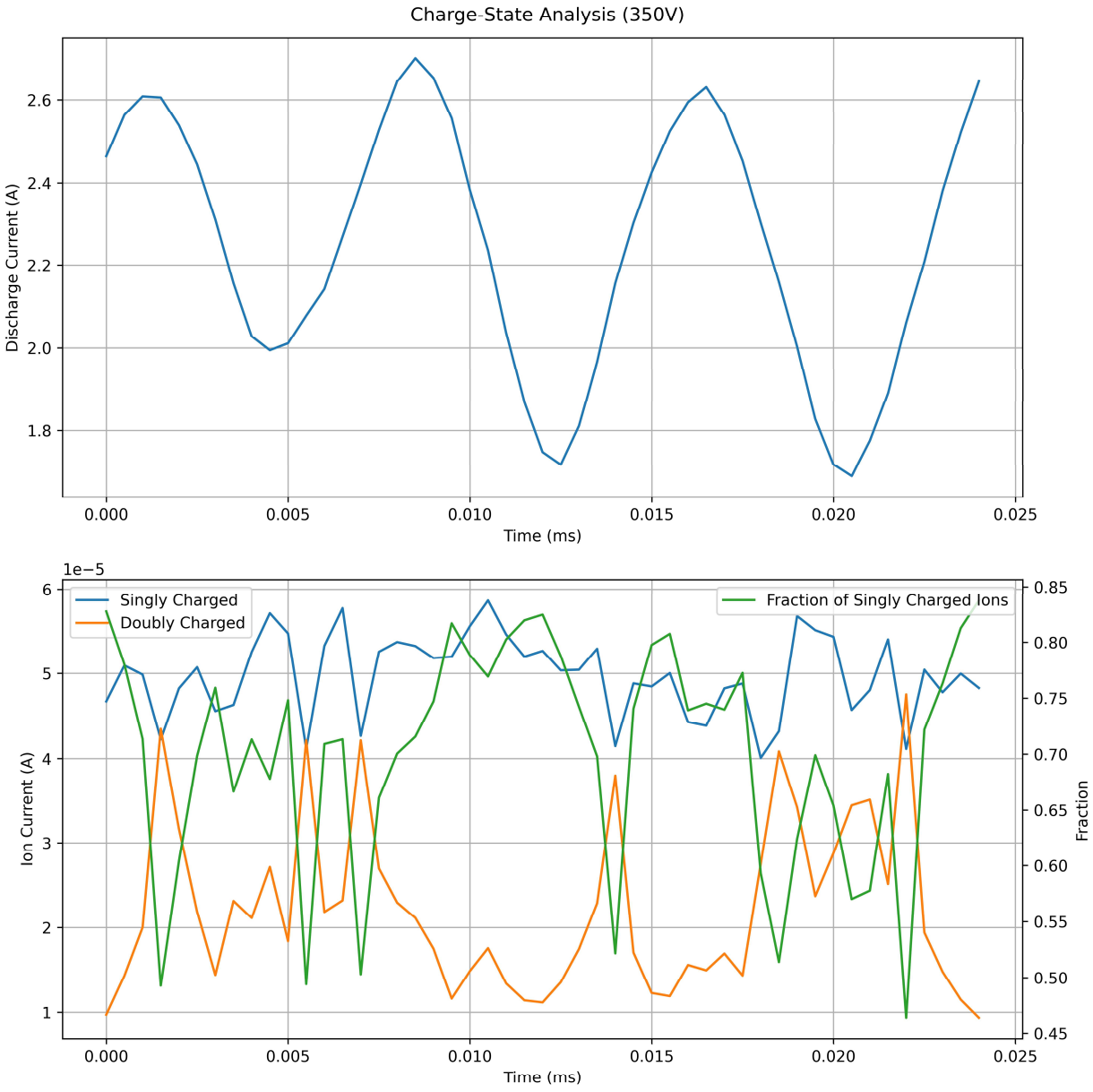

Figure IV-17: Results of charge-state analysis based on the curve-fitting to amplified reconstructed ExB probe measurements.

One can observe that ion current due to doubly charged ions varies approximately inversely to the ion current due to singly charged ions. As a result, the fraction of charge-state shows an oscillatory variation with high amplitude. The peak-to-peak amplitude of variation of the current fraction of singly charged ions reaches nearly 40%. However, the nature of correspondence of variation between the current fraction and the discharge current is unclear from this analysis. Large temporal oscillation of the current fraction implies the presence large variation of charge-state in the plasma along the axial direction of the exhaust plasma.

V. Conclusions

1. Summary of findings

The data-synchronization algorithm based on Fourier transfer functions and Fast-Fourier Transformation was applied for the first time to obtain time-resolved ExB probe measurements of Hall-thruster exhaust plasma operating on krypton at three operating conditions.

In each operating condition, it was confirmed through time-averaged analysis of the ExB probe measurement that the ion velocity distribution function has at least two peaks within the velocity range of interest. The time-averaged measurements were well characterized by the two-peak Maxwellian profile, which was used as the curve-fitting form throughout the investigation. Some irregularity was consistently observed for all three operating conditions between the primary peak (singly charged ions) and the secondary peak (doubly charged ions).

In the lowest power level ($V_d = 250\text{V}$) and the highest power level ($V_d = 350\text{V}$) tested, the discharge current oscillation was mostly dominated by a single-frequency sinusoidal oscillation. In the former case, the dominant frequency was around 25kHz, and around 125kHz in the latter

case. In these cases, the algorithm was applied to the specific dominant frequency and the synchronization of the measurements resulted in reasonable data. In both two cases, it was observe that the secondary peak shows stronger correspondence to the discharge current oscillation than the primary peak. This is explicable by the hypothesis that the generation mechanism of secondary charged ions is also influenced by the oscillatory behavior of the thruster, in addition to the fundamental acceleration mechanism common to both charge states.

The primary peak was only weakly influenced by the low-frequency oscillation seen in $V_d = 250\text{V}$, but showed strong correspondence to the high-frequency oscillation seen in $V_d = 350\text{V}$.

The use of picoammeter for ExB probe signal measurement most likely resulted in significant attenuation of the perceived probe signal. An artificial amplification was attempted in post-processing by amplifying the signal's deviation from the time-averaged data.

With $V_d = 250\text{V}$ and $V_d = 350\text{V}$, the numerical curve fitting with the reconstructed ExB measurement amplified by a factor of 10 is generally successful throughout the time domain of interest. The obtained best-fitting parameters with the two-peak Maxwellian distribution profile were then used to analyze the variation of charge-state distribution in response to the discharge current oscillations. In both cases, the analysis predicted significant variation in the charge-state distribution of plasma, more specifically the fraction of singly charged ions in the total ion current. With the amplification factor of 10, the peak-to-peak amplitude of oscillation of the ion current fraction of singly charged ions was estimated to be around 30~40%. The temporal variation of charge-state distribution indicates the presence of spatial variation of charge state in the axial direction of the exhaust plasma. The exact nature of correspondence between the charge state distribution and the discharge current oscillation remains unclear.

The oscillation of discharge current with $V_d = 300\text{V}$ contained distinct frequency components with approximately equal amplitudes. The synchronization was conducted for a band of frequencies. The results showed high amplitude oscillation of irregular plasma distribution between the primary and secondary peaks. It is unclear whether this phenomenon is physical or nonphysical. Curve-fitting largely resulted in nonphysical results likely due to the presence of irregularity.

2. Suggested future work

One major challenge with the design of the experimental setup for time-resolved ExB probe measurement was the device to convert ion current collected by the probe to voltage to be measured with an oscilloscope. The issue mainly arises from the frequency response of the device, as the device needs to be compatible with small, high-frequency current signal. A transimpedance amplifier (TIA) should be capable of such measurement, though the design of the TIA should be carefully considered.

Increasing the acquisition frequency and the size of the measurement will likely improve the algorithm's ability to better capture the physical behavior of the plasma. Some challenges for this improvement will be the data size and compatibility with computational data processing.

It is likely that one of the issues facing the numerical algorithm based on FFT and Fourier transfer functions was a deviation of the frequency components of the ExB probe signal from the discharge current oscillation. Some algorithms that do not rely on frequency analysis of the signals may overcome this specific challenge. One such algorithm is shadow manifold interpolation (SMI).

Some of the outcomes of this investigation leave important implications about the nature of the Hall thruster exhaust plasma but much of such outcomes remain qualitative due to the limitations with the experimental setup and methodology. However, the algorithm and approach laid out in this investigation can serve as the baseline for future research into the time-resolved behavior of ion velocity and charge-state distributions of Hall thruster plasma.

REFERENCES

[1] R. Shastry, R. R. Hofer, B. M. Reid, and A. D. Gallimore, "Method for analyzing E×B probe spectra from Hall thruster plumes," *Rev. Sci. Instrum.*, vol. 80, no. 6, p. 063502, Jun. 2009, doi: 10.1063/1.3152218.

[2] J. Anderson, "Charge-Exchange Collision Effect on ExB-probe location for NEXIS Testing," Jet Propulsion Laboratory, Jan. 16, 2004.

[3] B. Reid, R. Shastry, A. Gallimore, and R. Hofer, "Angularly-Resolved ExB Probe Spectra in the Plume of a 6-kW Hall Thruster," in *44th AIAA/ASME/SAE/ASEE Joint Propulsion Conference & Exhibit*, Hartford, CT: American Institute of Aeronautics and Astronautics, Jul. 2008. doi: 10.2514/6.2008-5287.

[4] H. Kim, Y. Lim, W. Choe, and J. Seon, "Effect of multiply charged ions on the performance and beam characteristics in annular and cylindrical type Hall thruster plasmas," *Appl. Phys. Lett.*, vol. 105, no. 14, p. 144104, Oct. 2014, doi: 10.1063/1.4897948.

[5] R. B. Lobbia, "A Time-resolved Investigation of the Hall Thruster Breathing Mode".

[6] D. Eckhardt, J. Koo, R. Martin, M. Holmes, and K. Hara, "Spatiotemporal data fusion and manifold reconstruction in Hall thrusters," *Plasma Sources Sci. Technol.*, vol. 28, no. 4, p. 045005, Apr. 2019, doi: 10.1088/1361-6595/ab0b1f.

[7] V. H. Chaplin *et al.*, "Time-resolved ion velocity measurements in a high-power Hall thruster using laser-induced fluorescence with transfer function averaging," *Appl. Phys. Lett.*, vol. 116, no. 23, p. 234107, Jun. 2020, doi: 10.1063/5.0007161.

[8] I. Romadanov, Y. Raitses, A. Diallo, K. Hara, I. D. Kaganovich, and A. Smolyakov, "On limitations of laser-induced fluorescence diagnostics for xenon ion velocity distribution function measurements in Hall thrusters," *Phys. Plasmas*, vol. 25, no. 3, p. 033501, Mar. 2018, doi: 10.1063/1.5020749.

[9] A. Ortega, "Numerical Simulations for the Assessment of Erosion in the 12.5-kW Hall Effect Rocket with Magnetic Shielding (HERMeS)," presented at the 35th International Electric Propulsion Conference, 10/82017.

[10] S. Ha, "Erosion and Performance Scaling of Electrodeless Plasma Thrusters with a Magnetic Nozzle".

[11] M. L. Hause, B. D. Prince, and R. J. Bemish, "Krypton charge exchange cross sections for Hall effect thruster models," *J. Appl. Phys.*, vol. 113, no. 16, p. 163301, Apr. 2013, doi: 10.1063/1.4802432.

[12] P. Thoreau and J. Little, "Influence of Field Topology on Magnetically Shielded Hall Thruster Plume Divergence," in *2022 IEEE Aerospace Conference (AERO)*, Mar. 2022, pp. 1–8. doi: 10.1109/AERO53065.2022.9843247.